

**Visual Computing and
AI Department**

4D and Quantum
Vision Group $\langle \mathcal{A} | \psi \rangle$
Motus • Quanta • Visus

SIC Lecture Series

01.09.2021

3D Computer Vision: From a Classical to a Quantum Perspective

SIC Lecture Series (01.09.2021)

Vladislav Golyanik

4D and Quantum
Vision Group



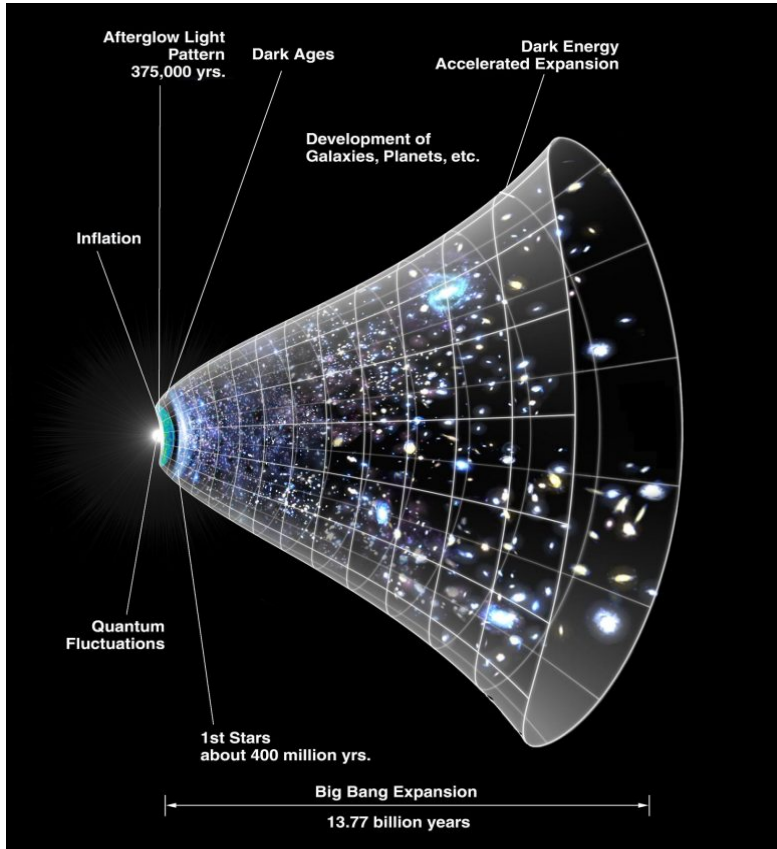
Visual Computing and
AI Department

Outline

- Introduction
- Overview of the Research Fields (4DQV Group)
- Adiabatic Quantum Computing
- Quantum Algorithms for Computer Vision and Graphics

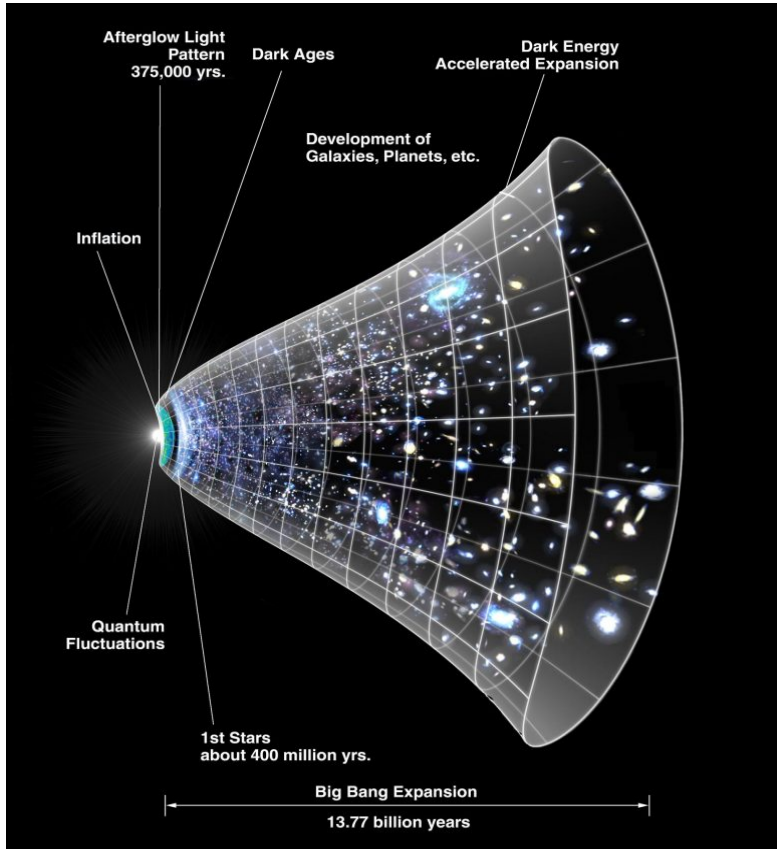
Why 3D+t?

Why 3D+t?

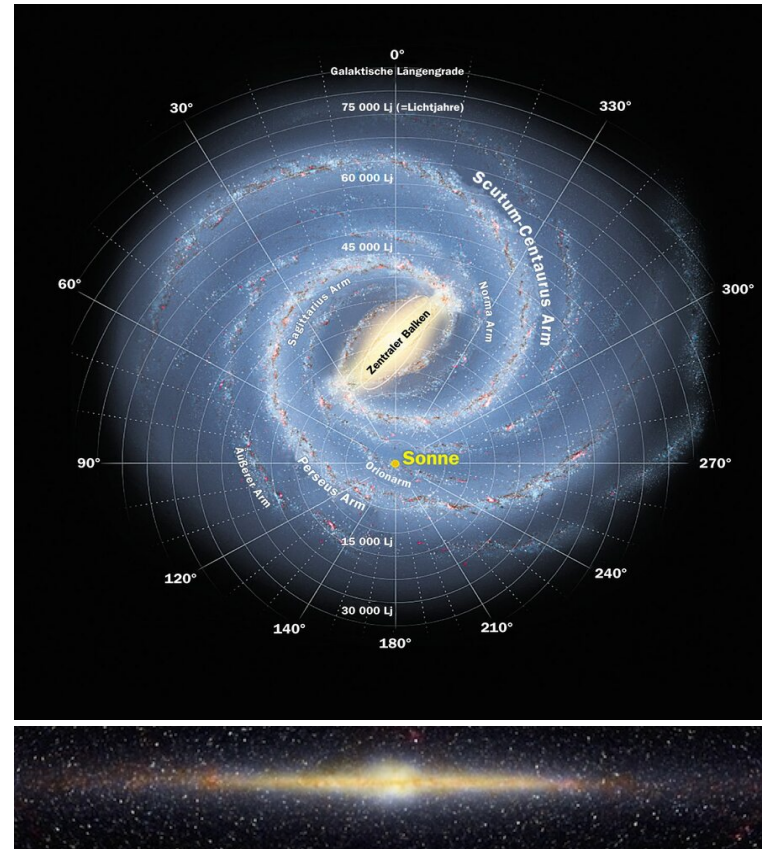


Expansion of the universe

Why 3D+t?

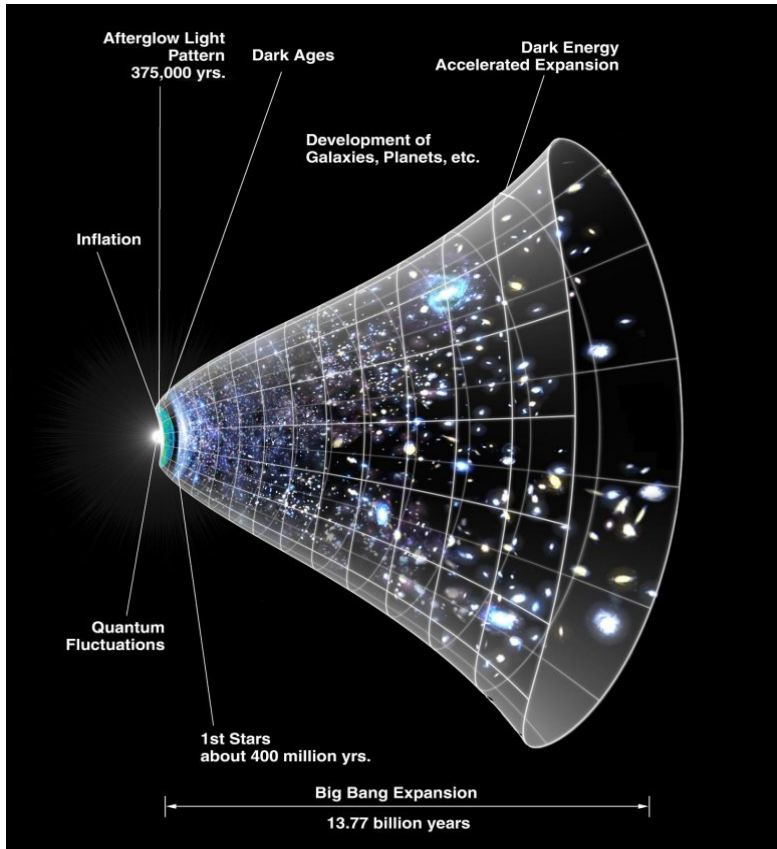


Expansion of the universe

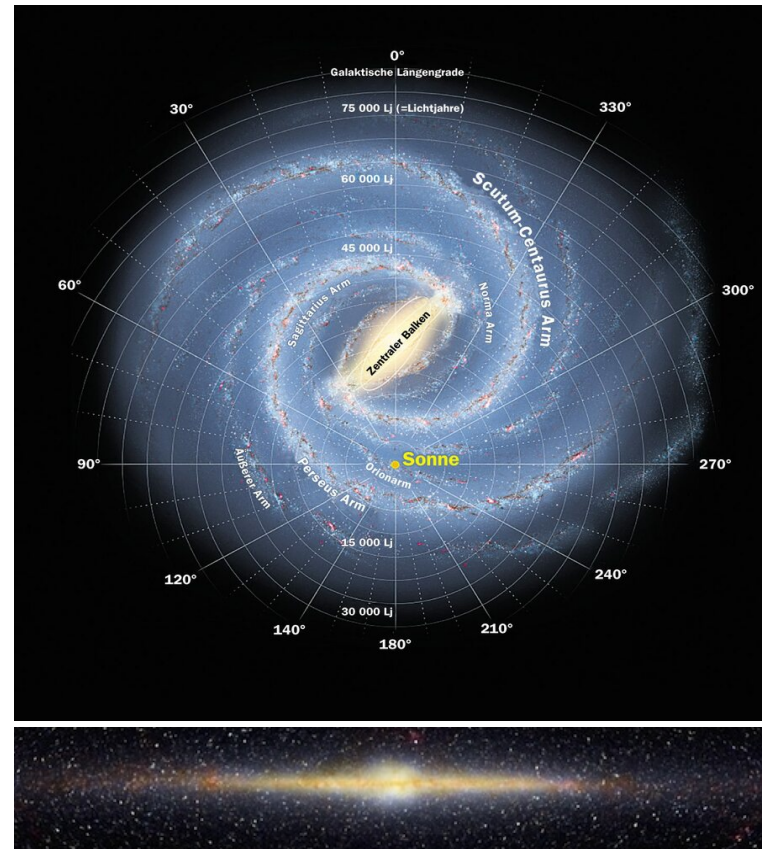


The Milky Way

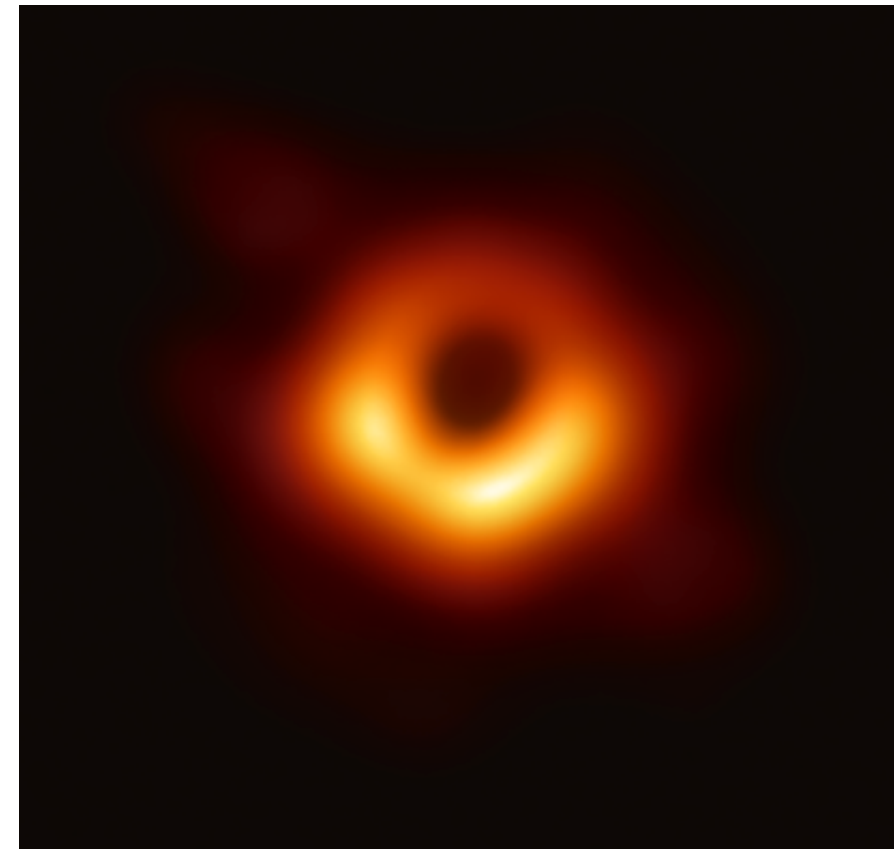
Why 3D+t?



Expansion of the universe



The Milky Way



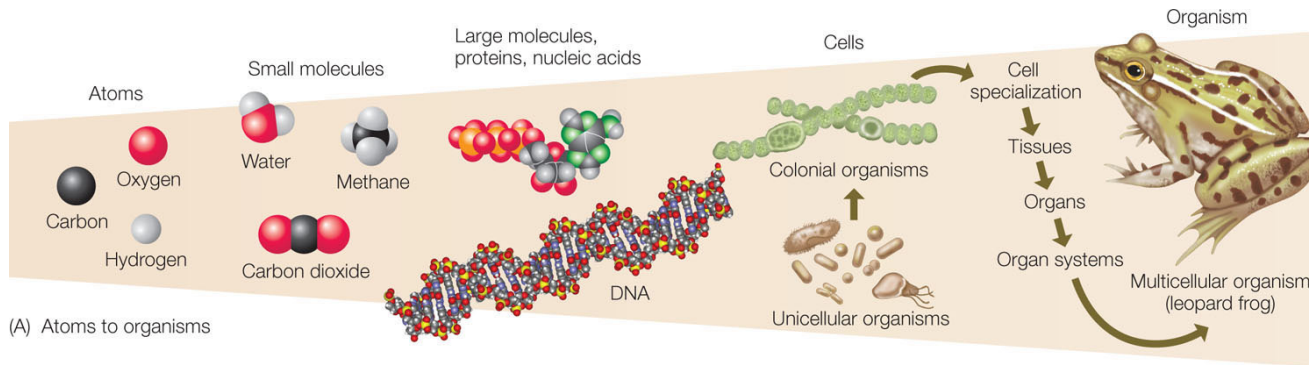
Black Hole M87*

The history of the universe is, in effect, a huge and ongoing quantum computation. The universe is a quantum computer.

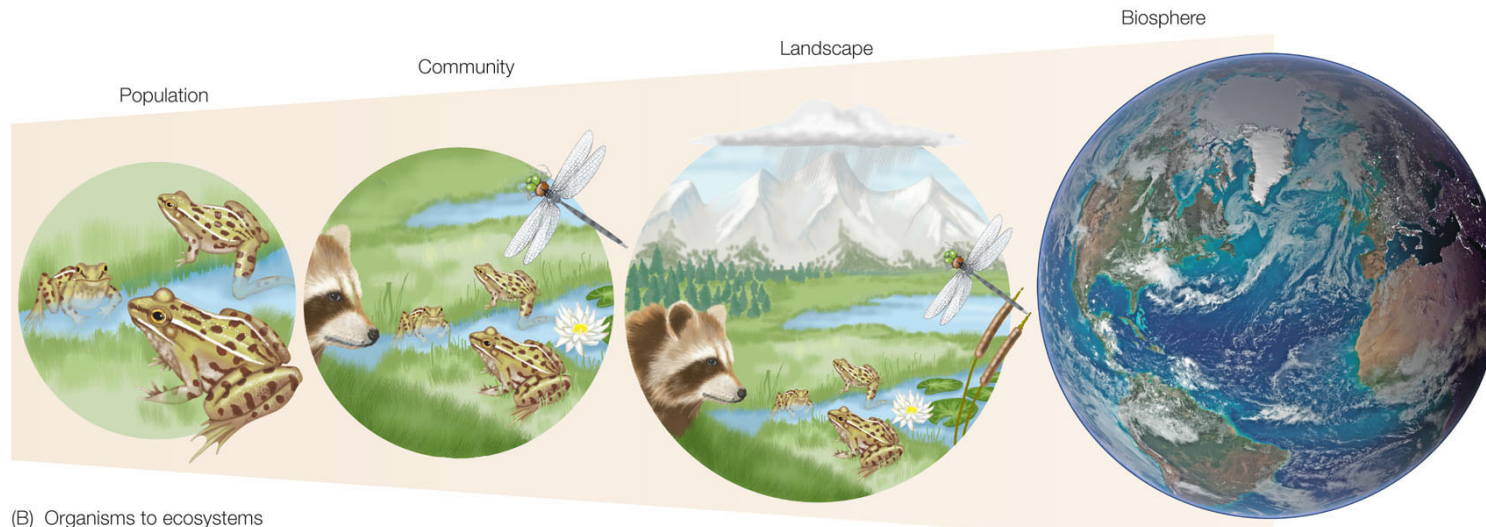
Seth Lloyd

Vladislav Golyanik

Why 3D+t?



(A) Atoms to organisms

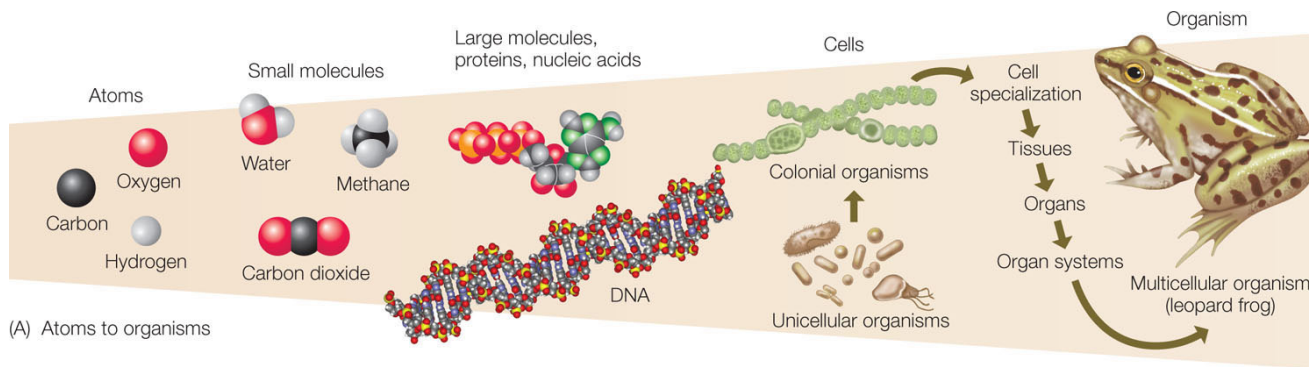


(B) Organisms to ecosystems

1.5 *Biosphere*: NASA images by Reto Stöckli, based on data from NASA and NOAA.

Tewari *et al.* High-Fidelity Monocular Face Reconstruction based on an Unsupervised Model-based Face Autoencoder. TPAMI, 2017.
 Parot *et al.* Photometric Stereo Endoscopy. Journal of Biomedical Optics, 2013.
 Golyanik *et al.* Introduction to Coherent Depth Fields for Dense Monocular Surface Recovery. BMVC, 2017.

Why 3D+t?



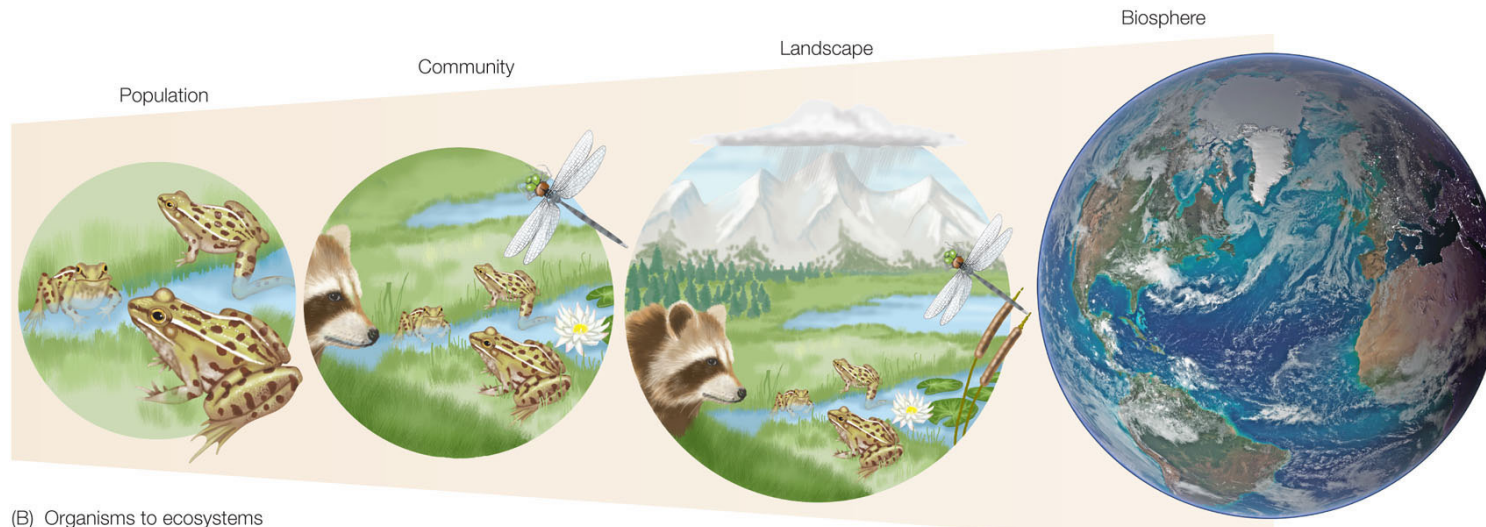
(A) Atoms to organisms



Sports



HCI (Gesture recognition)



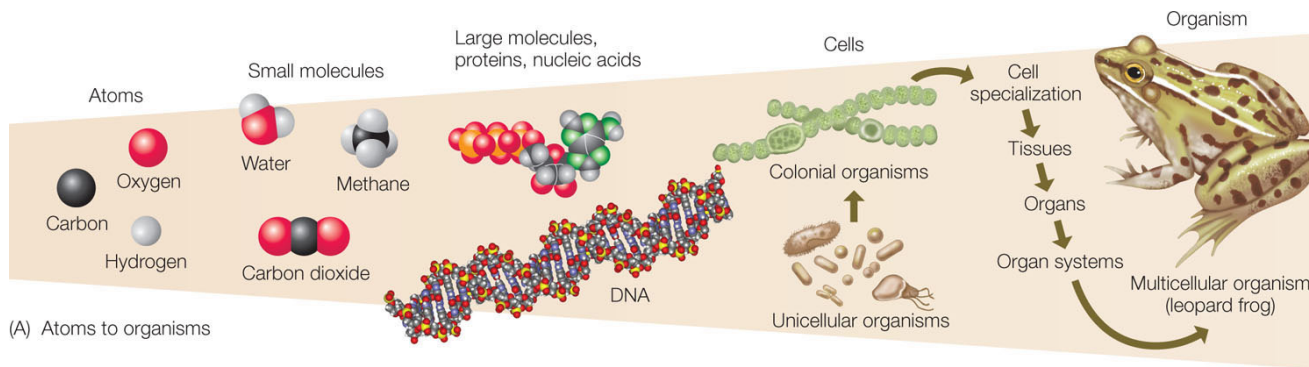
(B) Organisms to ecosystems

1.5 *Biosphere*: NASA images by Reto Stöckli, based on data from NASA and NOAA.

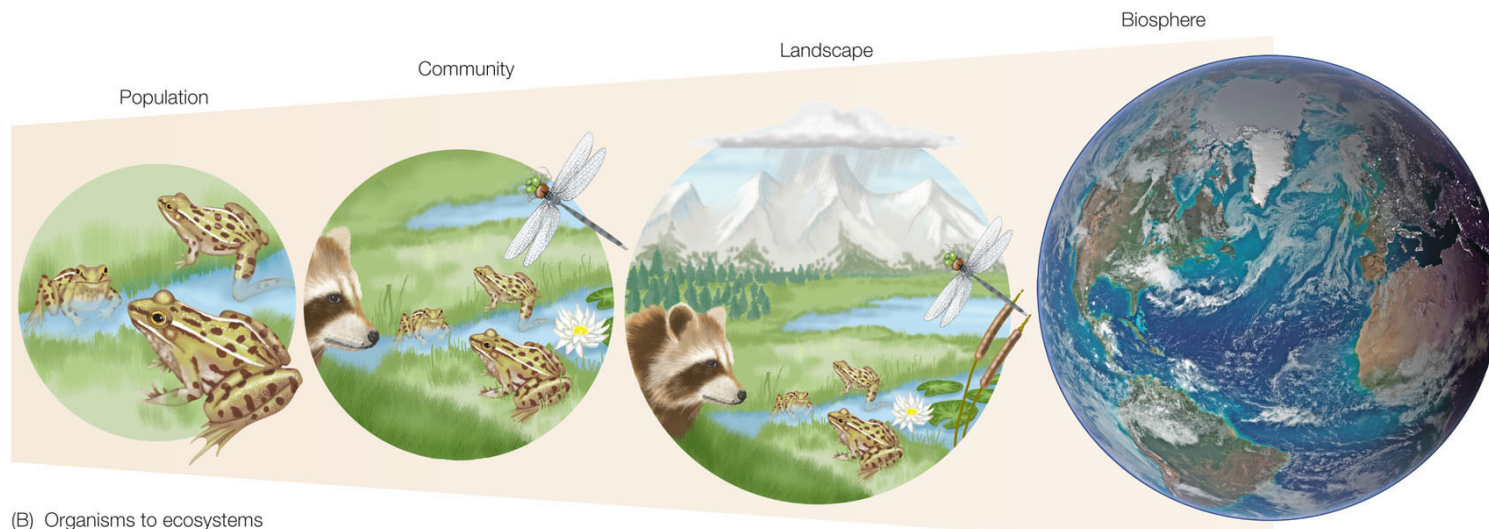
Tewari *et al.* High-Fidelity Monocular Face Reconstruction based on an Unsupervised Model-based Face Autoencoder. TPAMI, 2017.
Parot *et al.* Photometric Stereo Endoscopy. Journal of Biomedical Optics, 2013.
Golyanik *et al.* Introduction to Coherent Depth Fields for Dense Monocular Surface Recovery. BMVC, 2017.

Vladislav Golyanik

Why 3D+t?



(A) Atoms to organisms



(B) Organisms to ecosystems

1.5 *Biosphere*: NASA images by Reto Stöckli, based on data from NASA and NOAA.



Sports

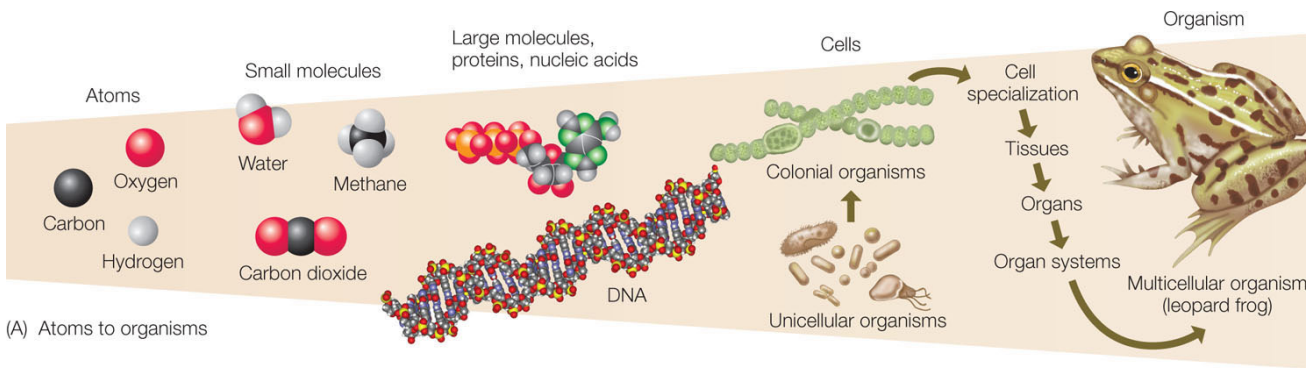


HCI (Gesture recognition)

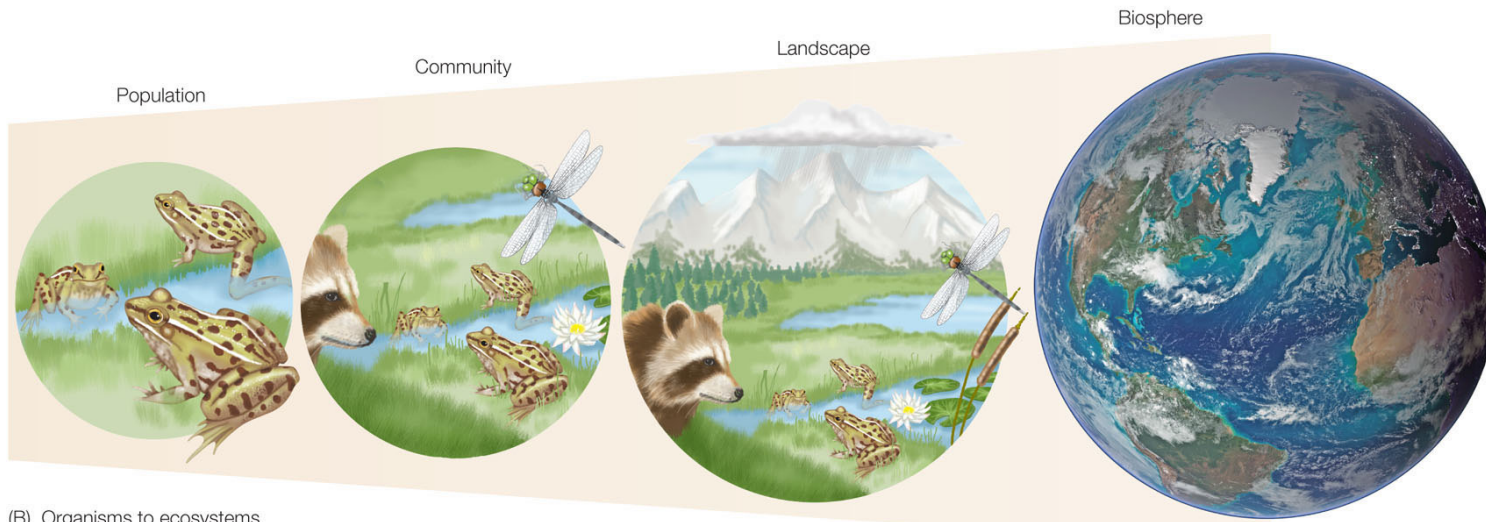


Human face and body parts (e.g., back)

Why 3D+t?



(A) Atoms to organisms



(B) Organisms to ecosystems

1.5 *Biosphere*: NASA images by Reto Stöckli, based on data from NASA and NOAA.



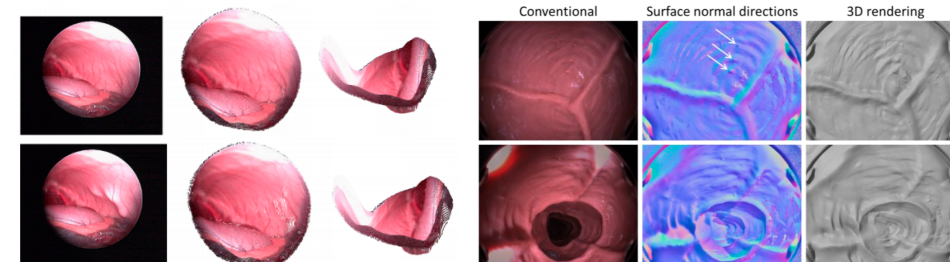
Sports



HCI (Gesture recognition)



Human face and body parts (e.g., back)

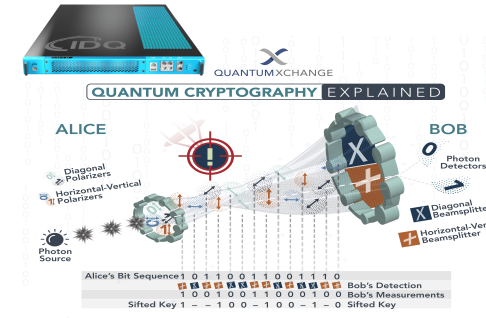
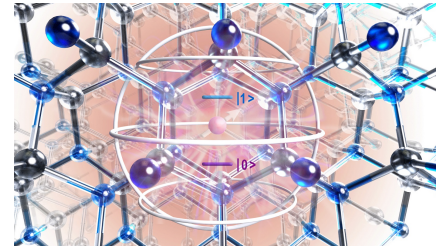
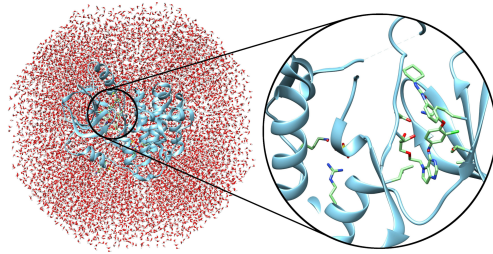
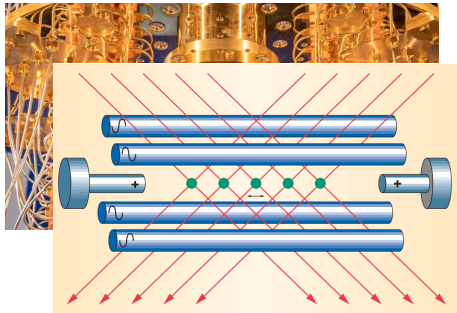


Endoscopic videos

Tewari *et al.* High-Fidelity Monocular Face Reconstruction based on an Unsupervised Model-based Face Autoencoder. TPAMI, 2017.
 Parot *et al.* Photometric Stereo Endoscopy. Journal of Biomedical Optics, 2013.
 Golyanik *et al.* Introduction to Coherent Depth Fields for Dense Monocular Surface Recovery. BMVC, 2017.

Vladislav Golyanik

Applications of Quantum Computing



Material science

Drug discovery

Quantum cryptography



Machine learning



SECURITY MEASURES FOR THE QUANTUM AGE

Boosters:

- Theoretically obtained results are promising
- Broad interest of scientific community and industry
- Progress in physical hardware realisations
- Investments

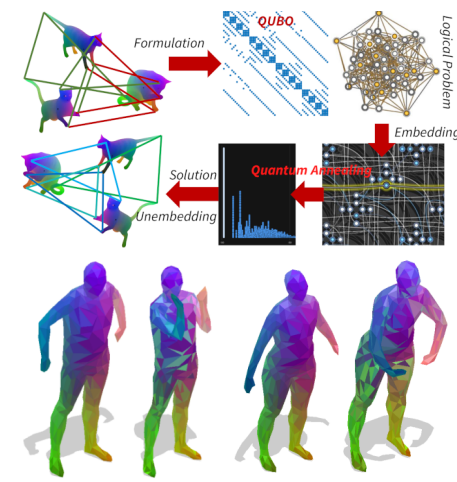
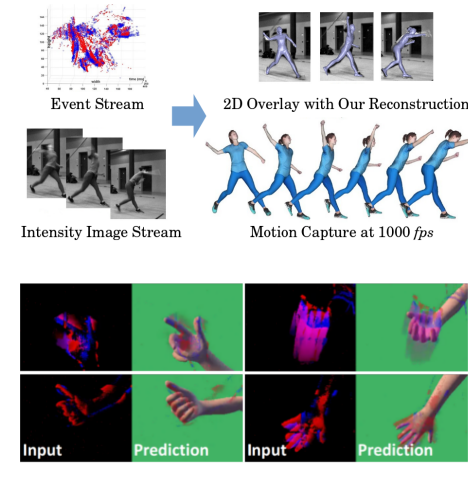
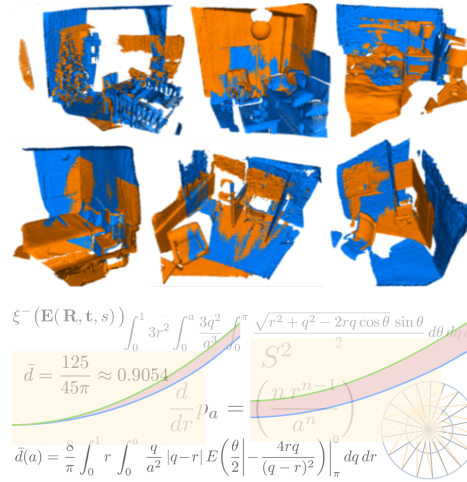
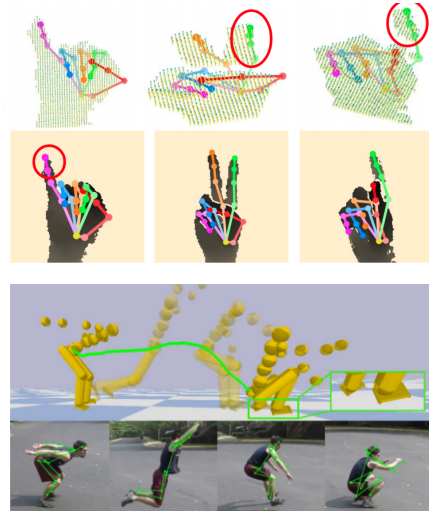
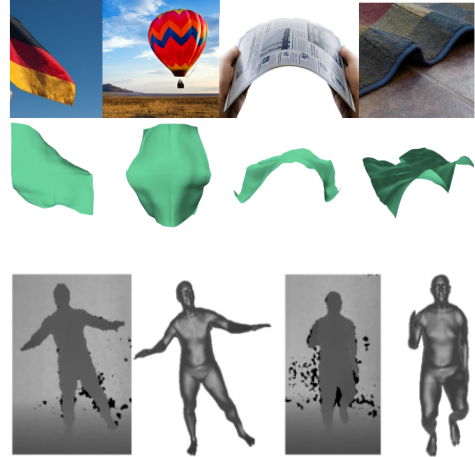
Applications:

- Material science
- Drug research
- Cryptography
- Machine learning

+ many others

...

Overview: 4DQV Group (D6)



4D reconstruction
(general non-rigid scenes)

4D reconstruction
(hand and humans)

Point cloud analysis
(alignment)

Event-based vision
(non-rigid scenes)

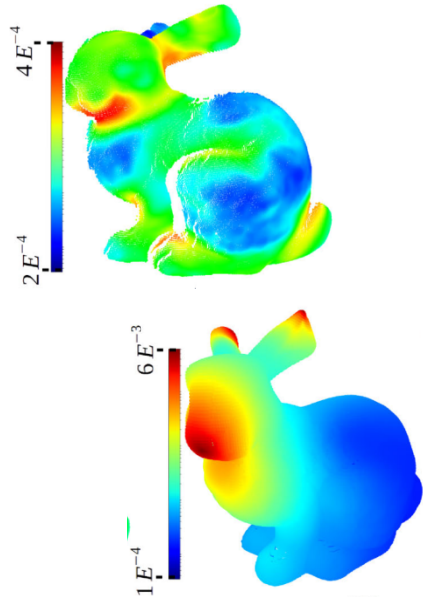
Quantum CV

- 4D reconstruction and tracking of non-rigid scenes and objects
- Neural rendering
- Point set registration and other matching problems
- Event-based approaches in vision and graphics
- Quantum algorithms for computer vision and graphics

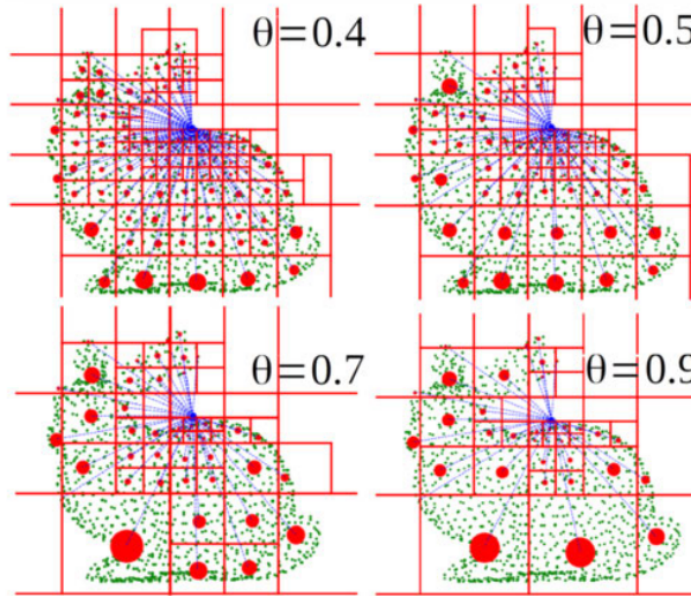


Neural rendering (implicit 3D)

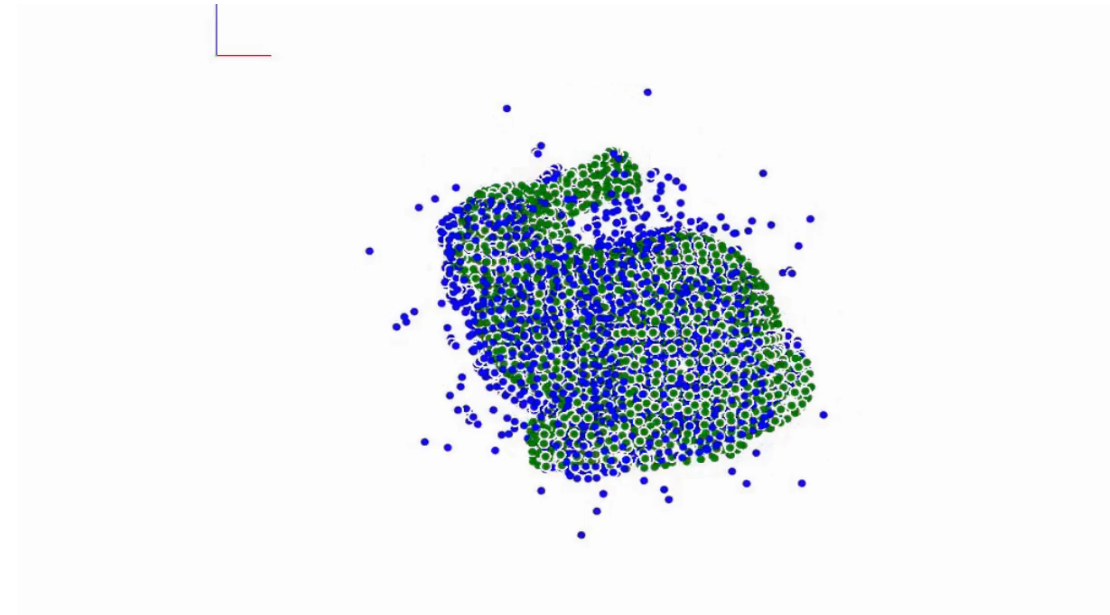
Fast Gravitational Approach (FGA)



Pointwise features mapped to masses



Barnes-Hut 2^D -tree



Alignment iterations (FGA)

Gravitational Potential Energy (GPE) of the system:
$$\mathbf{E}(\mathbf{R}, \mathbf{t}) = -G \sum_{i,j} \frac{m_{\mathbf{Y}_i} m_{\mathbf{X}_j}}{(\|\mathbf{R}\mathbf{r}_{\mathbf{Y}_i} + \mathbf{t} - \mathbf{r}_{\mathbf{X}_j}\| + \epsilon)}$$

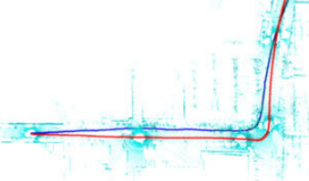
Alignment of LIDAR Data

Avg. runtime (CPU) - 75.8 sec.
Avg. runtime (GPU) - 0.81 sec.
Avg. iterations/registration - 36
#Points(M+N) per frame - 234.2k
#registration pairs - 153



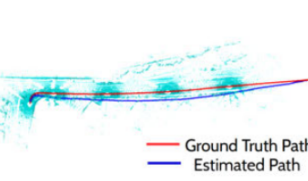
(a). 2011_09_26_drive_0005 Seq.

Avg. runtime (CPU) - 70.3 sec
Avg. runtime (GPU) - 0.79 sec.
Avg. iterations/registration - 32
#Points(M+N) per frame - 232.1k
#registration pairs - 446



(b). 2011_09_26_drive_0009 Seq.

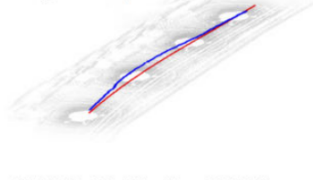
Avg. runtime (CPU) - 67.28 sec
Avg. runtime (GPU) - 0.65 sec.
Avg. iterations/registration - 34
#Points(M+N) per frame: 224.4k
#registration pairs - 313



(c). 2011_09_26_drive_0014 Seq.

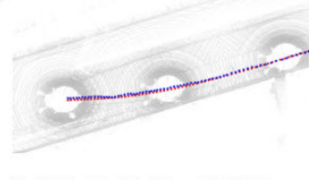


Avg. runtime (GPU) - 1.08 sec.
Avg. iterations - 58
#Points(M+N) per frame - 202.8k
#registration pairs - 107



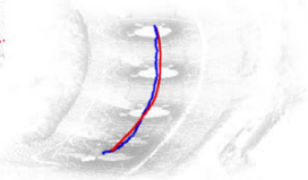
(d). 2011_09_26_drive_0001 Seq.

Avg. runtime (GPU) - 0.71 sec.
Avg. iterations - 39
#Points(M+N) per frame - 230.7k
#registration pairs - 76

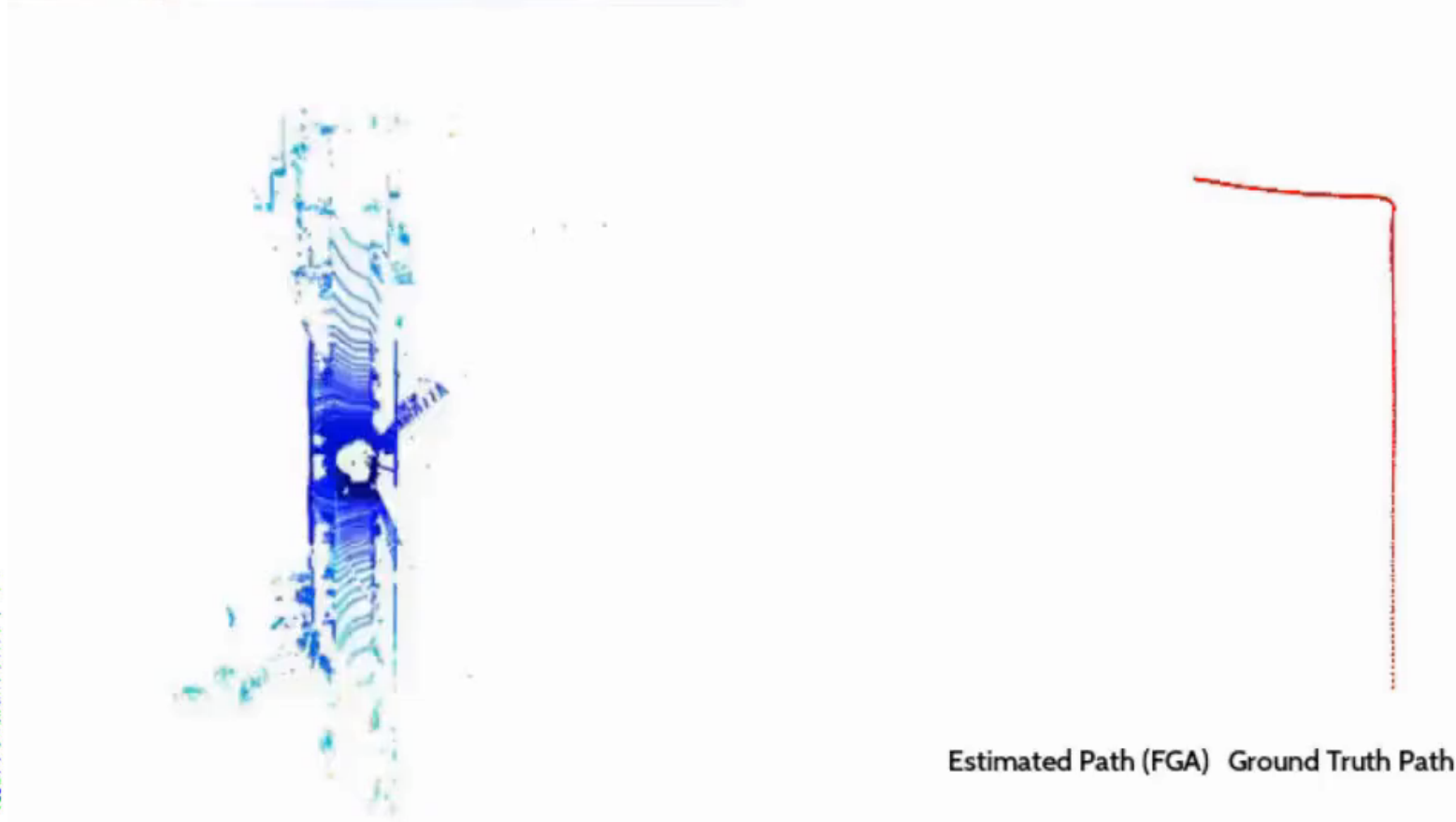


(e). 2011_09_26_drive_0002 Seq.

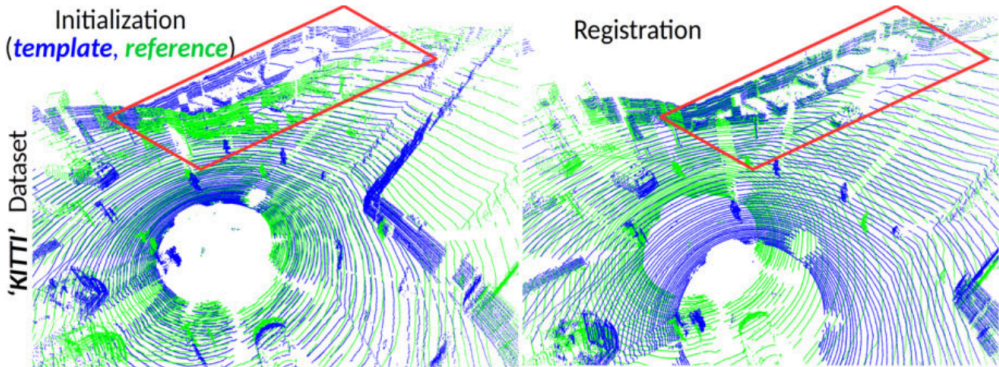
Avg. runtime (GPU) - 1.35 sec.
Avg. iterations - 90
#Points(M+N) per frame - 221.4k
#registration pairs - 232



(f). 2011_09_26_drive_0011 Seq.

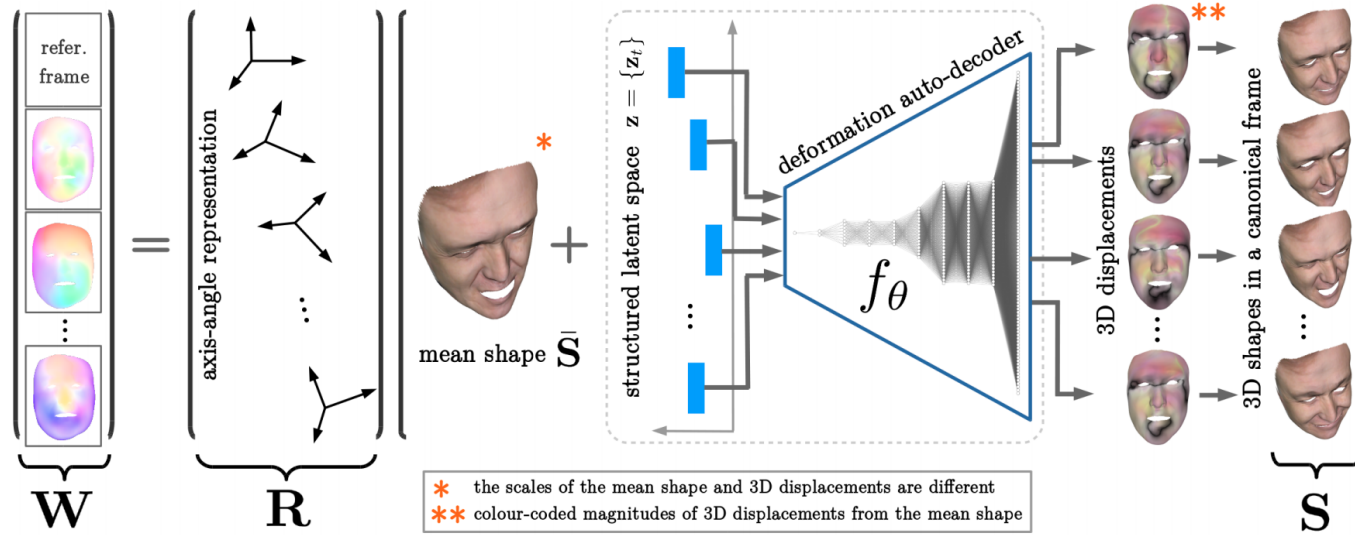


Estimated Path (FGA) Ground Truth Path



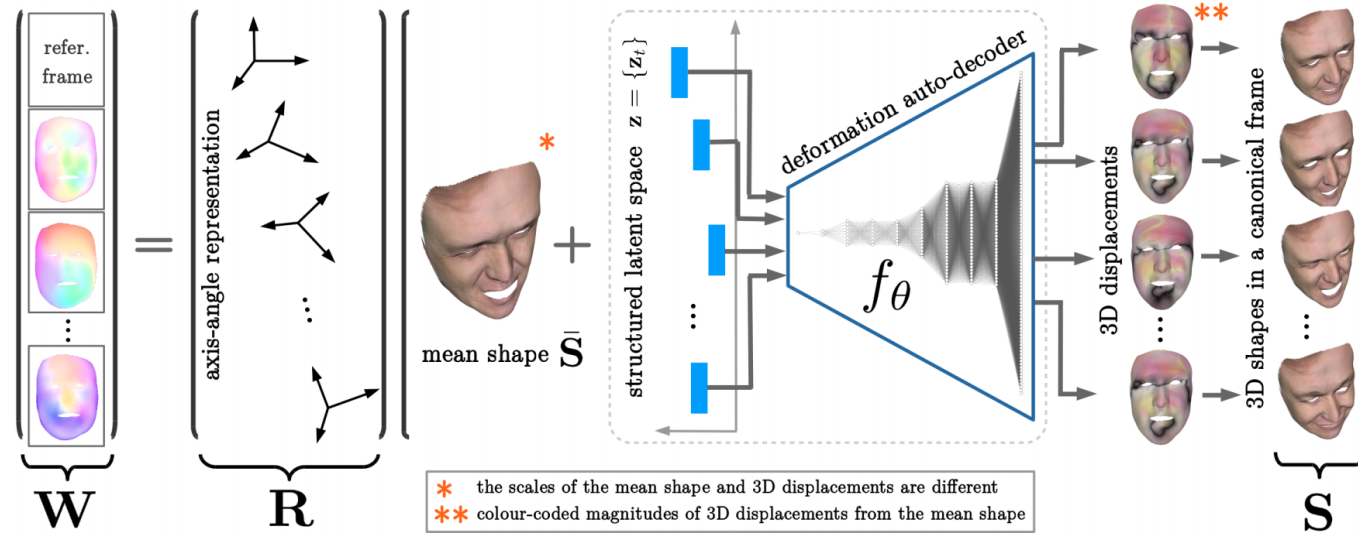
Path Estimation using the sensor poses (T^*) obtained while registering consecutive frames

Neural Dense NRSfM



Overview of neural dense NRSfM with latent space constraints

Neural Dense NRSfM

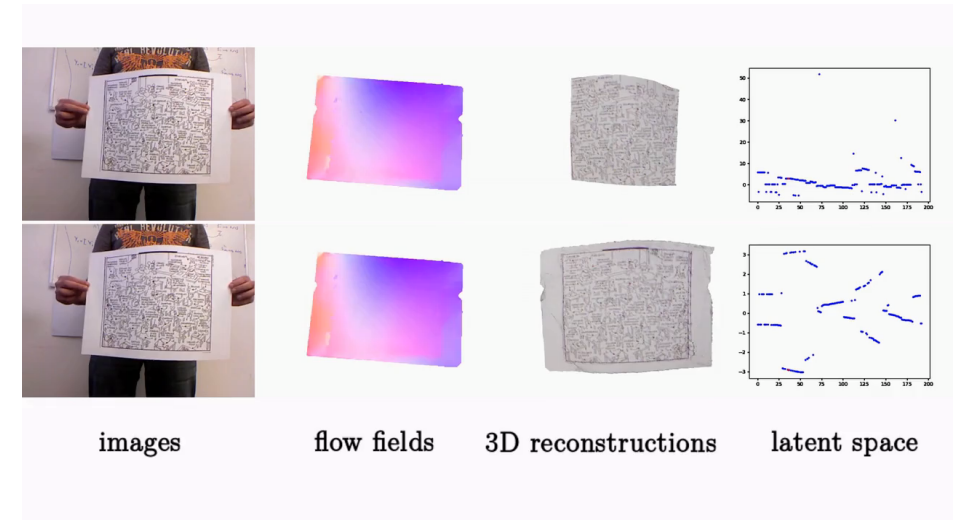


Overview of neural dense NRSfM with latent space constraints

Sparsity constraints on the latent space function:

$$\mathbf{E}_{\text{latent}}(\mathbf{z}) = \|\mathcal{F}(\mathbf{z})\|_1$$

- Dense NRSfM is worth studying because the principles are applicable to many other (more well-posed) problems
- Results of dense NRSfM serve as a “lower bound” for many other problems

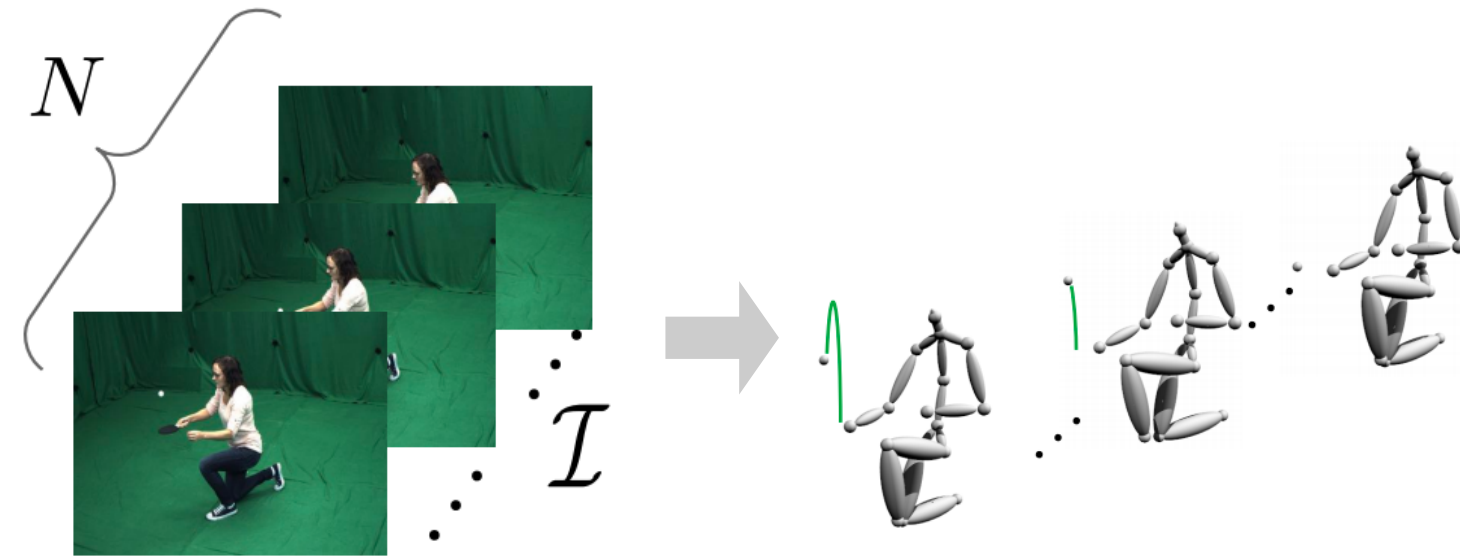


3D reconstructions of *Kinect t-shirt* and *paper* sequences



optical flow colour scheme

GraviCap



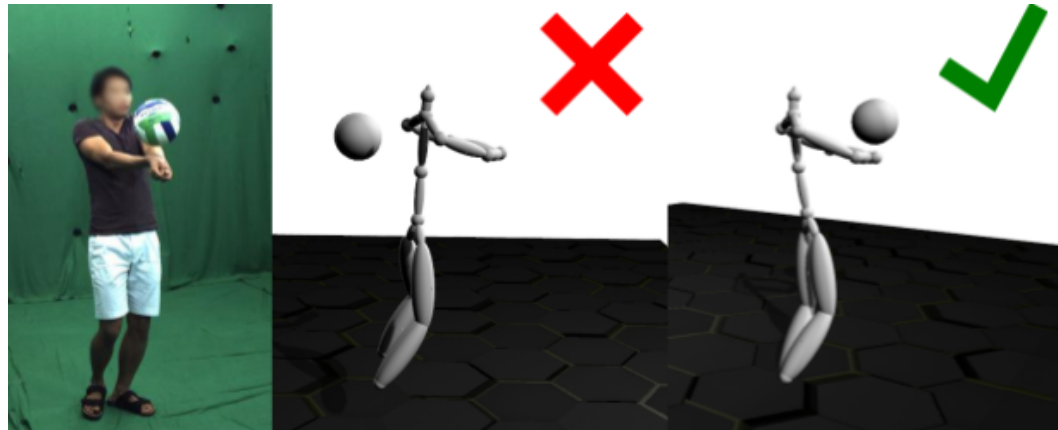
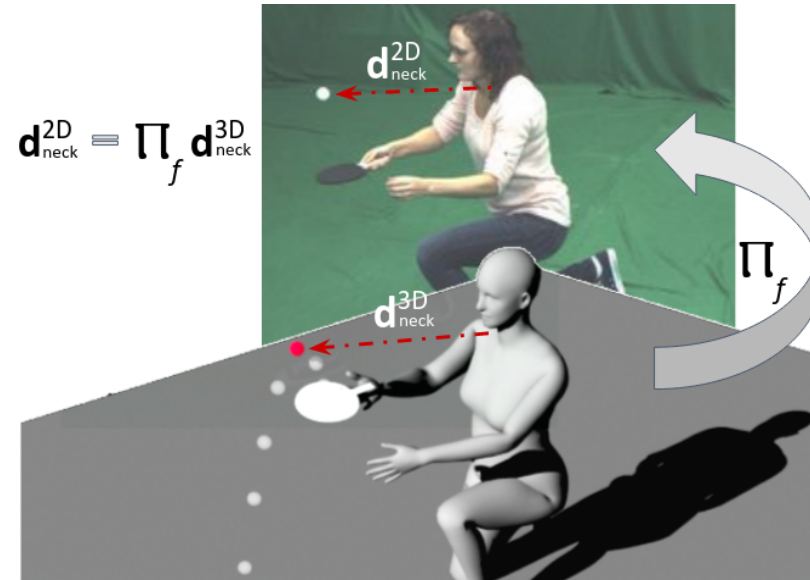
Input 2D images

3D reconstructions
(human and object)



Input videos and the corresponding 3D reconstructions

GraviCap



$$x_i = f \frac{X_i}{Z_i} + c_x, y_i = f \frac{Y_i}{Z_i} + c_y, \forall i,$$

$$\text{s. t. } \sqrt{g_x^2 + g_y^2 + g_z^2} = 9.81 \text{ m/s}^2,$$

$$\text{where } \begin{cases} X_i = X_0 + u_x t + \frac{1}{2} g_x t^2, \\ Y_i = Y_0 + u_y t + \frac{1}{2} g_y t^2, \text{ and} \\ Z_i = Z_0 + u_z t + \frac{1}{2} g_z t^2. \end{cases}$$



Dabral, Shimada, Jain, Theobalt, Golyanik. Gravity-Aware Monocular 3D Human-Object Reconstruction. *ICCV*, 2021.

Vladislav Golyanik

EventHands



inivation
DAVIS 240C

2021 **ICCV** OCTOBER 11-17
VIRTUAL

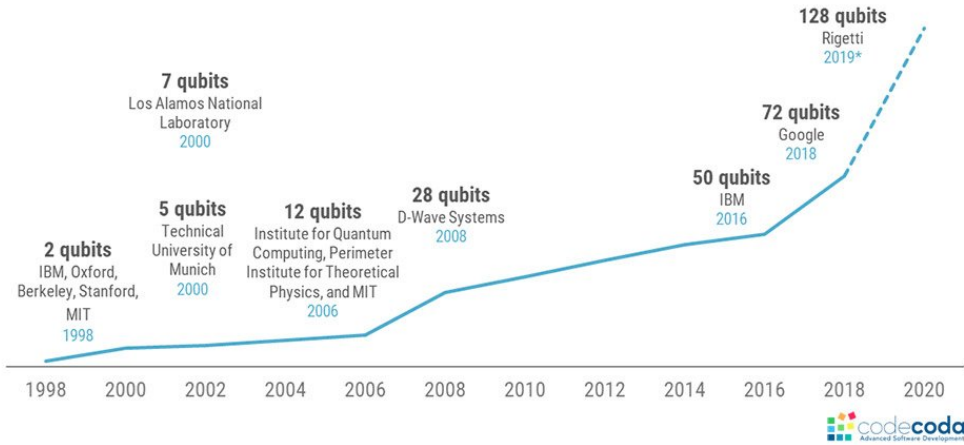
Playback speed: 0.5x

Rudnev, Golyanik, Wang, Mueller, Seidel, Elgharib, Theobalt. EventHands: Real-Time Neural 3D Hand Pose Estimation from an Event Stream. *ICCV*, 2021.

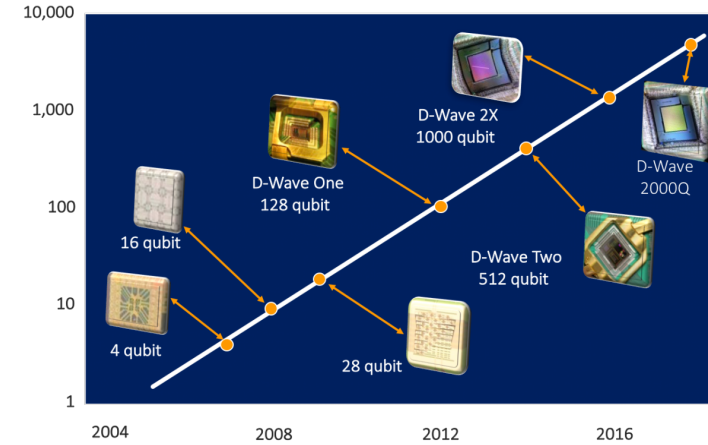
Part II: Changing the Perspective

- Introduction
- Overview of the Research Fields (4DQV Group)
- Adiabatic Quantum Computing
- Quantum Algorithms for Computer Vision and Graphics

Circuit-Based vs Adiabatic Model

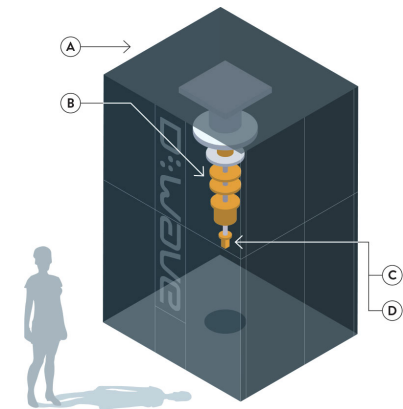


qubits (all QC types)



qubits and AQC generations (D-Wave)

	Circuit-based QC	Adiabatic QC (Quantum Annealers)
type	Universal	Specialised
can solve	All classical and quantum algorithms (for the circuit-based model)	QUBO/Ising problems
number of qubits	up to 27	>5000 (35000 couplers)

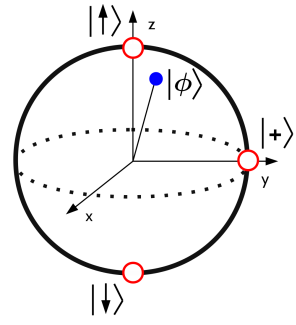


Operations on Qubits

complex numbers



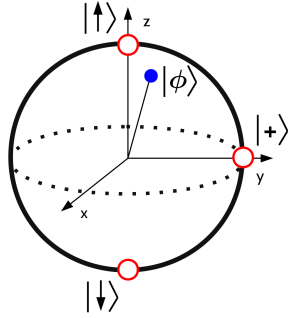
$$|\psi\rangle = \alpha |0\rangle + \beta |1\rangle$$



Operations on Qubits

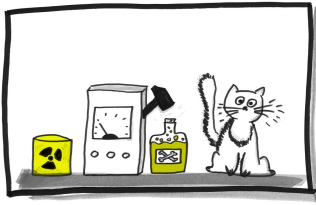
complex numbers

$$|\psi\rangle = \alpha |0\rangle + \beta |1\rangle$$



Born's rule:

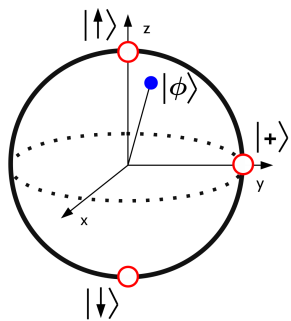
$|\alpha|^2$ to obtain $|0\rangle$
 $|\beta|^2$ to obtain $|1\rangle$



Operations on Qubits

complex numbers

$$|\psi\rangle = \alpha |0\rangle + \beta |1\rangle$$



Bra-Ket (Dirac) notation:

$$|0\rangle = \begin{bmatrix} 1 \\ 0 \end{bmatrix} \quad |1\rangle = \begin{bmatrix} 0 \\ 1 \end{bmatrix}$$

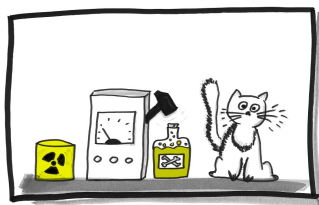
$$\langle 0| = [1 \quad 0] \quad \langle 1| = [0 \quad 1]$$

$$\langle q_1 | q_2 \rangle = [\alpha \quad \beta] \begin{bmatrix} \eta \\ \zeta \end{bmatrix} = \alpha\eta + \beta\zeta$$

Born's rule:

$|\alpha|^2$ to obtain $|0\rangle$

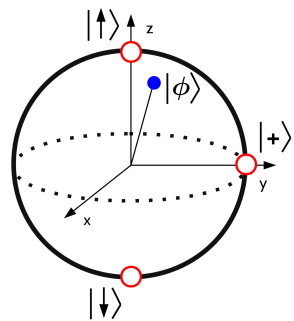
$|\beta|^2$ to obtain $|1\rangle$



Operations on Qubits

complex numbers

$$|\psi\rangle = \alpha |0\rangle + \beta |1\rangle$$



Bra-Ket (Dirac) notation:

$$|0\rangle = \begin{bmatrix} 1 \\ 0 \end{bmatrix} \quad |1\rangle = \begin{bmatrix} 0 \\ 1 \end{bmatrix}$$

$$\langle 0| = [1 \quad 0] \quad \langle 1| = [0 \quad 1]$$

$$\langle q_1 | q_2 \rangle = [\alpha \quad \beta] \begin{bmatrix} \eta \\ \zeta \end{bmatrix} = \alpha\eta + \beta\zeta \quad |\phi\rangle = \alpha |00\rangle + \beta |01\rangle + \eta |10\rangle + \zeta |11\rangle$$

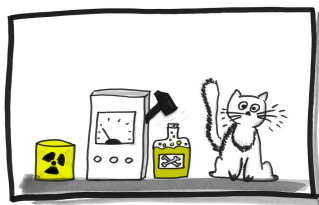
Hilbert spaces (2^n -dimensional vector spaces):

$$|0\rangle \otimes |1\rangle = |01\rangle = \begin{bmatrix} 1 \\ 0 \end{bmatrix} \otimes \begin{bmatrix} 0 \\ 1 \end{bmatrix} = \begin{bmatrix} 0 \\ 1 \\ 0 \\ 0 \end{bmatrix} \quad |00\rangle = \begin{bmatrix} 1 \\ 0 \\ 0 \\ 0 \end{bmatrix} \quad |10\rangle = \begin{bmatrix} 0 \\ 0 \\ 1 \\ 0 \end{bmatrix} \quad |11\rangle = \begin{bmatrix} 0 \\ 0 \\ 0 \\ 1 \end{bmatrix}$$

Born's rule:

$|\alpha|^2$ to obtain $|0\rangle$

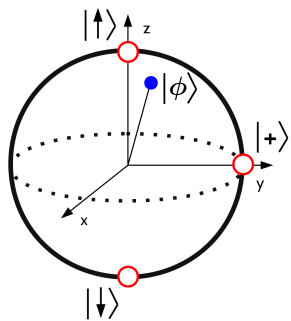
$|\beta|^2$ to obtain $|1\rangle$



Operations on Qubits

complex numbers

$$|\psi\rangle = \alpha |0\rangle + \beta |1\rangle$$



Bra-Ket (Dirac) notation:

$$|0\rangle = \begin{bmatrix} 1 \\ 0 \end{bmatrix} \quad |1\rangle = \begin{bmatrix} 0 \\ 1 \end{bmatrix}$$

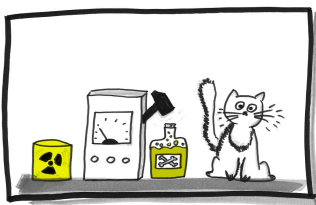
$$\langle 0| = [1 \quad 0] \quad \langle 1| = [0 \quad 1]$$

Hilbert spaces (2^n -dimensional vector spaces):

$$|0\rangle \otimes |1\rangle = |01\rangle = \begin{bmatrix} 1 \\ 0 \end{bmatrix} \otimes \begin{bmatrix} 0 \\ 1 \end{bmatrix} = \begin{bmatrix} 0 \\ 1 \\ 0 \\ 0 \end{bmatrix} \quad |00\rangle = \begin{bmatrix} 1 \\ 0 \\ 0 \\ 0 \end{bmatrix} \quad |10\rangle = \begin{bmatrix} 0 \\ 0 \\ 1 \\ 0 \end{bmatrix} \quad |11\rangle = \begin{bmatrix} 0 \\ 0 \\ 0 \\ 1 \end{bmatrix}$$

Born's rule:

$|\alpha|^2$ to obtain $|0\rangle$
 $|\beta|^2$ to obtain $|1\rangle$



$$\langle q_1 | q_2 \rangle = [\alpha \quad \beta] \begin{bmatrix} \eta \\ \zeta \end{bmatrix} = \alpha\eta + \beta\zeta \quad |\phi\rangle = \alpha |00\rangle + \beta |01\rangle + \eta |10\rangle + \zeta |11\rangle$$

QC is a form of reversible computing:

$$H = \frac{1}{\sqrt{2}} \begin{pmatrix} 1 & 1 \\ 1 & -1 \end{pmatrix} \quad CNOT = CX = \begin{bmatrix} 1 & 0 & 0 & 0 \\ 0 & 1 & 0 & 0 \\ 0 & 0 & 0 & 1 \\ 0 & 0 & 1 & 0 \end{bmatrix}$$

* acts on a single qubit

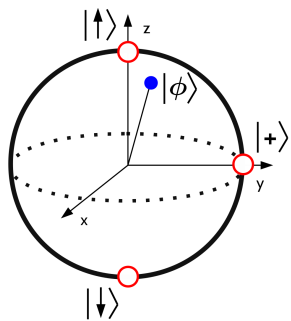
* acts on two qubits

- No loss of information
- Unitary matrices preserving vector lengths

Operations on Qubits

complex numbers

$$|\psi\rangle = \alpha |0\rangle + \beta |1\rangle$$



Bra-Ket (Dirac) notation:

$$|0\rangle = \begin{bmatrix} 1 \\ 0 \end{bmatrix} \quad |1\rangle = \begin{bmatrix} 0 \\ 1 \end{bmatrix}$$

$$\langle 0| = [1 \quad 0] \quad \langle 1| = [0 \quad 1]$$

$$\langle q_1 | q_2 \rangle = [\alpha \quad \beta] \begin{bmatrix} \eta \\ \zeta \end{bmatrix} = \alpha\eta + \beta\zeta \quad |\phi\psi\rangle = \alpha |00\rangle + \beta |01\rangle + \eta |10\rangle + \zeta |11\rangle$$

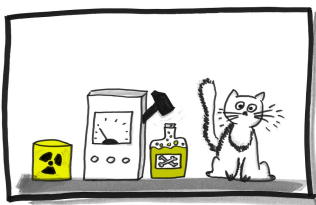
Hilbert spaces (2^n -dimensional vector spaces):

$$|0\rangle \otimes |1\rangle = |01\rangle = \begin{bmatrix} 1 \\ 0 \end{bmatrix} \otimes \begin{bmatrix} 0 \\ 1 \end{bmatrix} = \begin{bmatrix} 0 \\ 1 \\ 0 \\ 0 \end{bmatrix} \quad |00\rangle = \begin{bmatrix} 1 \\ 0 \\ 0 \\ 0 \end{bmatrix} \quad |10\rangle = \begin{bmatrix} 0 \\ 0 \\ 1 \\ 0 \end{bmatrix} \quad |11\rangle = \begin{bmatrix} 0 \\ 0 \\ 0 \\ 1 \end{bmatrix}$$

Born's rule:

$|\alpha|^2$ to obtain $|0\rangle$

$|\beta|^2$ to obtain $|1\rangle$



QC is a form of reversible computing:

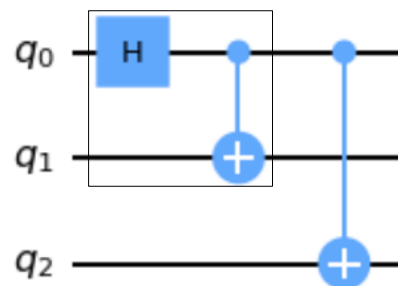
$$H = \frac{1}{\sqrt{2}} \begin{pmatrix} 1 & 1 \\ 1 & -1 \end{pmatrix}$$

$$CNOT = CX = \begin{bmatrix} 1 & 0 & 0 & 0 \\ 0 & 1 & 0 & 0 \\ 0 & 0 & 0 & 1 \\ 0 & 0 & 1 & 0 \end{bmatrix}$$

* acts on a single qubit

* acts on two qubits

Qubit entanglement:

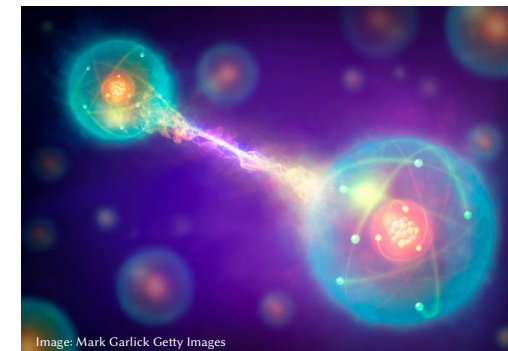


$$|\Phi^+\rangle = \frac{|00\rangle + |11\rangle}{\sqrt{2}}$$

Bell state

$$|\text{GHZ}\rangle = \frac{|000\rangle + |111\rangle}{\sqrt{2}}$$

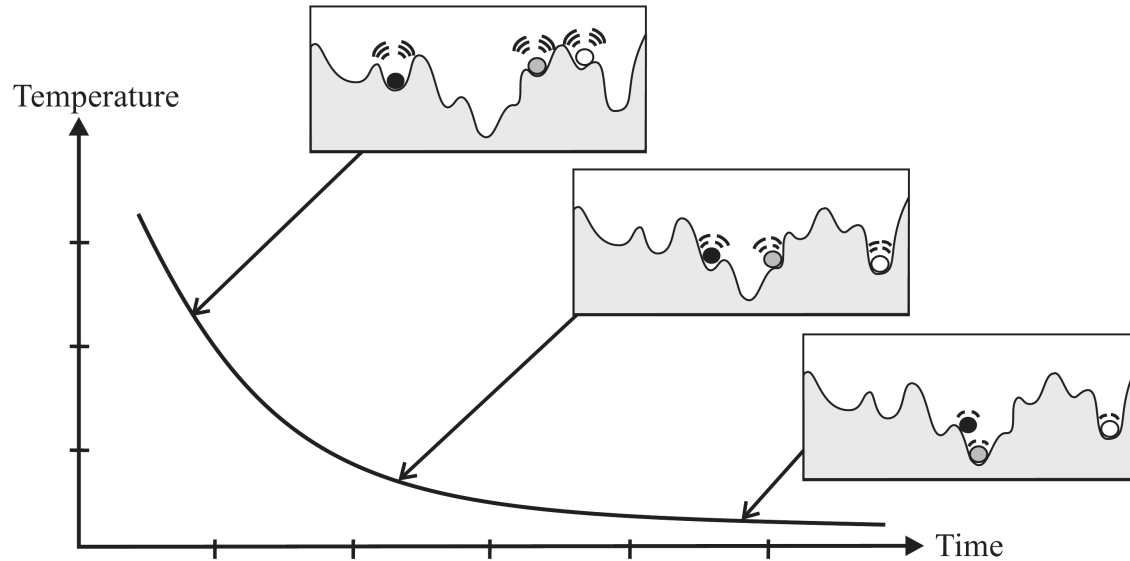
A three-qubit GHZ state



- No loss of information
- Unitary matrices preserving vector lengths

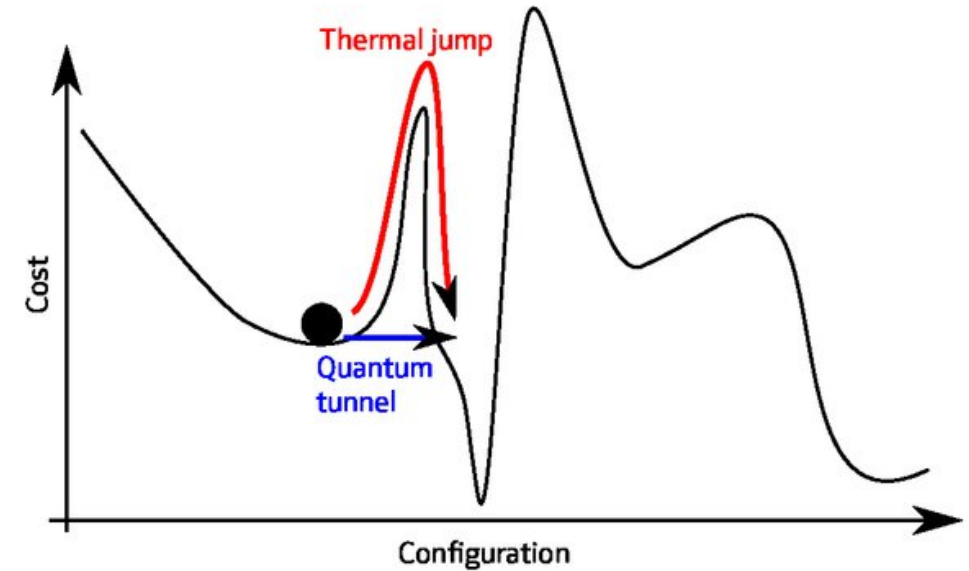
- Entangled particles *communicate* with each other instantaneously
- No *external* information can be passed when entangled particles affect each other

Simulated vs Quantum Annealing



Simulated Thermal Fluctuations

Main Parameter: Temperature



Quantum Fluctuations (physical phenomenon)

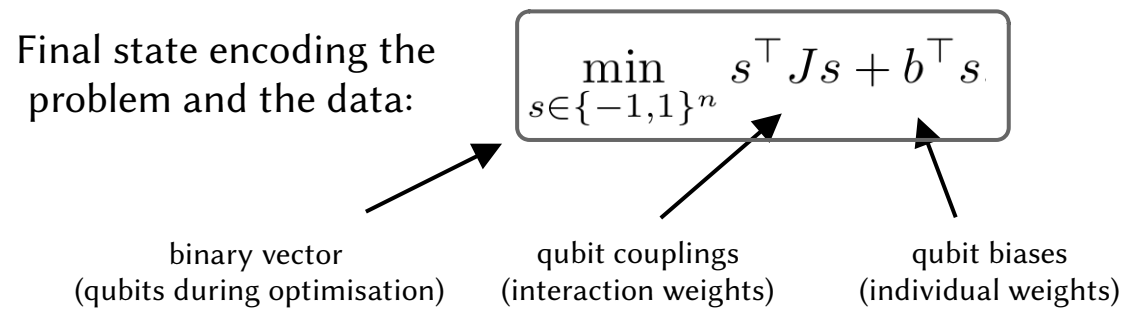
Main Parameter: Transverse Magnetic Field

Effects: Tunnelling, Superposition and Entanglement

Transition between Hamiltonians

Initial state: $|\psi(t = 0)\rangle = \bigotimes_{i=1}^n \frac{1}{\sqrt{2}} (|0\rangle + |1\rangle)$

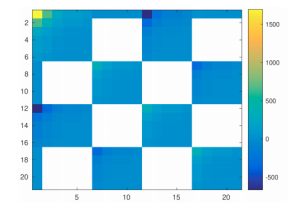
Transition (simplified): $H(t) = \left(1 - \frac{t}{\tau}\right) H_I + \frac{t}{\tau} H_P$



	q1	q2	q3
q1		0.7	1.9
q2	0.7		-0.3
q3	1.9	-0.3	

0.5 0.5 0.1

q1
q2
q3



Exemplary J (QUBO, 21 qubits)

Transition between Hamiltonians

Initial state: $|\psi(t = 0)\rangle = \bigotimes_{i=1}^n \frac{1}{\sqrt{2}} (|0\rangle + |1\rangle)$

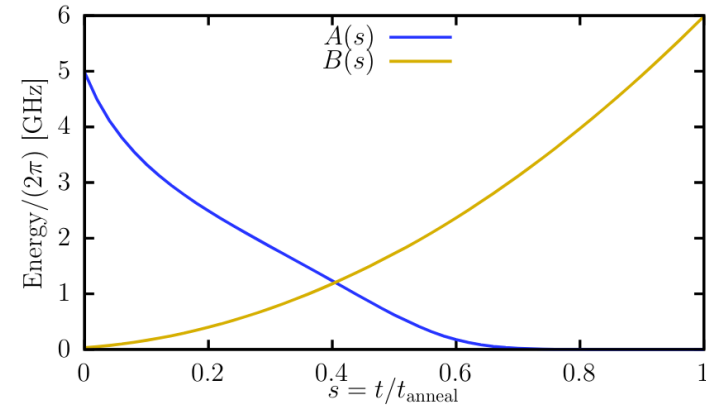
Transition (simplified): $H(t) = \left(1 - \frac{t}{\tau}\right) H_I + \frac{t}{\tau} H_P$

Final state encoding the problem and the data: $\min_{s \in \{-1,1\}^n} s^\top J s + b^\top s$

binary vector
(qubits during optimisation)

qubit couplings
(interaction weights)

qubit biases
(individual weights)

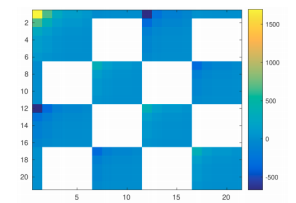


Annealing functions (schedules)

	q1	q2	q3
q1		0.7	1.9
q2	0.7		-0.3
q3	1.9	-0.3	

0.5 0.5 0.1

q1
q2
q3



Exemplary J (QUBO, 21 qubits)

Transition between Hamiltonians

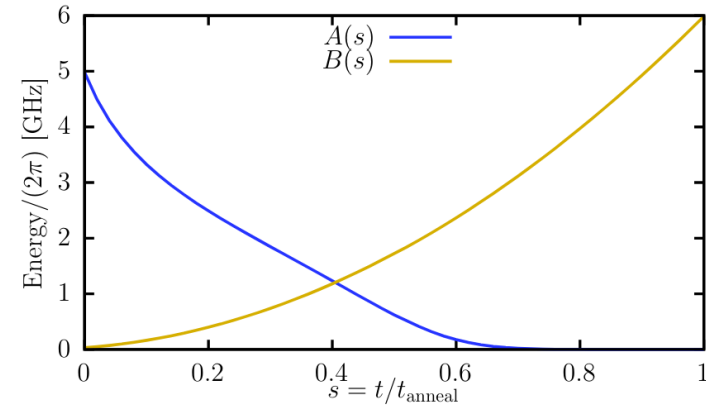
Initial state: $|\psi(t = 0)\rangle = \bigotimes_{i=1}^n \frac{1}{\sqrt{2}} (|0\rangle + |1\rangle)$

Transition (simplified): $H(t) = \left(1 - \frac{t}{\tau}\right) H_I + \frac{t}{\tau} H_P$

Final state encoding the problem and the data:

$$\min_{s \in \{-1, 1\}^n} s^T J s + b^T s$$

binary vector
(qubits during optimisation)
qubit couplings
(interaction weights)
qubit biases
(individual weights)



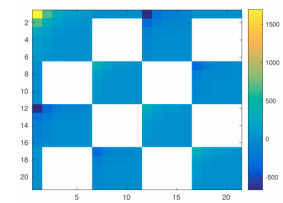
Annealing functions (schedules)

[Born and Fock, 1928]: *A physical system remains in its instantaneous eigenstate if a given perturbation is acting on it slowly enough and if there is a gap between the eigenvalue and the rest of the Hamiltonian's spectrum.*

	q1	q2	q3
q1		0.7	1.9
q2	0.7		-0.3
q3	1.9	-0.3	

0.5 0.5 0.1

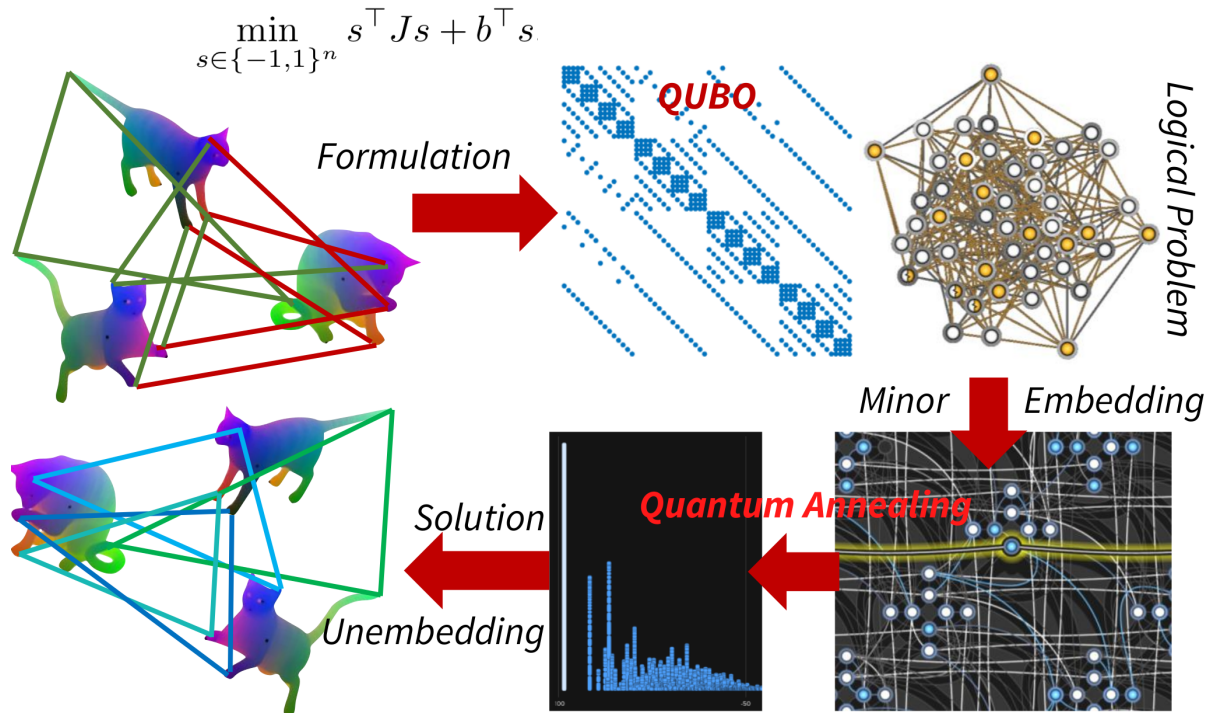
q1
q2
q3



Exemplary J (QUBO, 21 qubits)

[Manin, 1980][Feynman, 1982]: A quantum computer is proposed
 [Kadowaki and Nishimori, 1998]: Quantum annealing
 [Farhi *et al.*, 2001]: Quantum adiabatic evolution algorithm

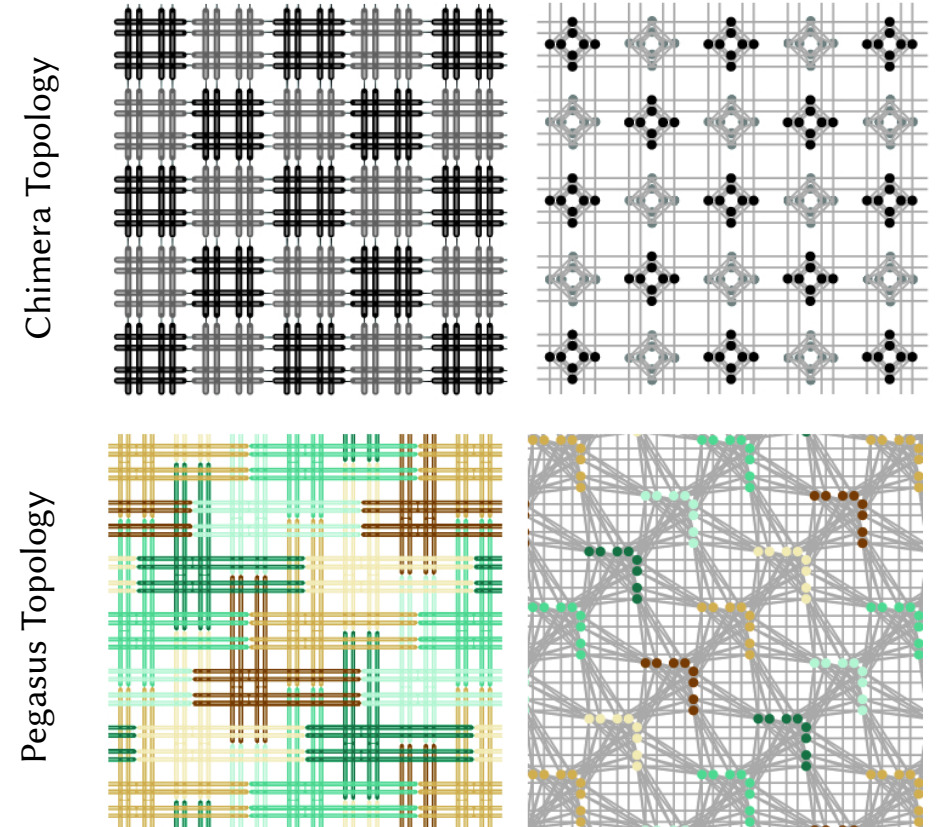
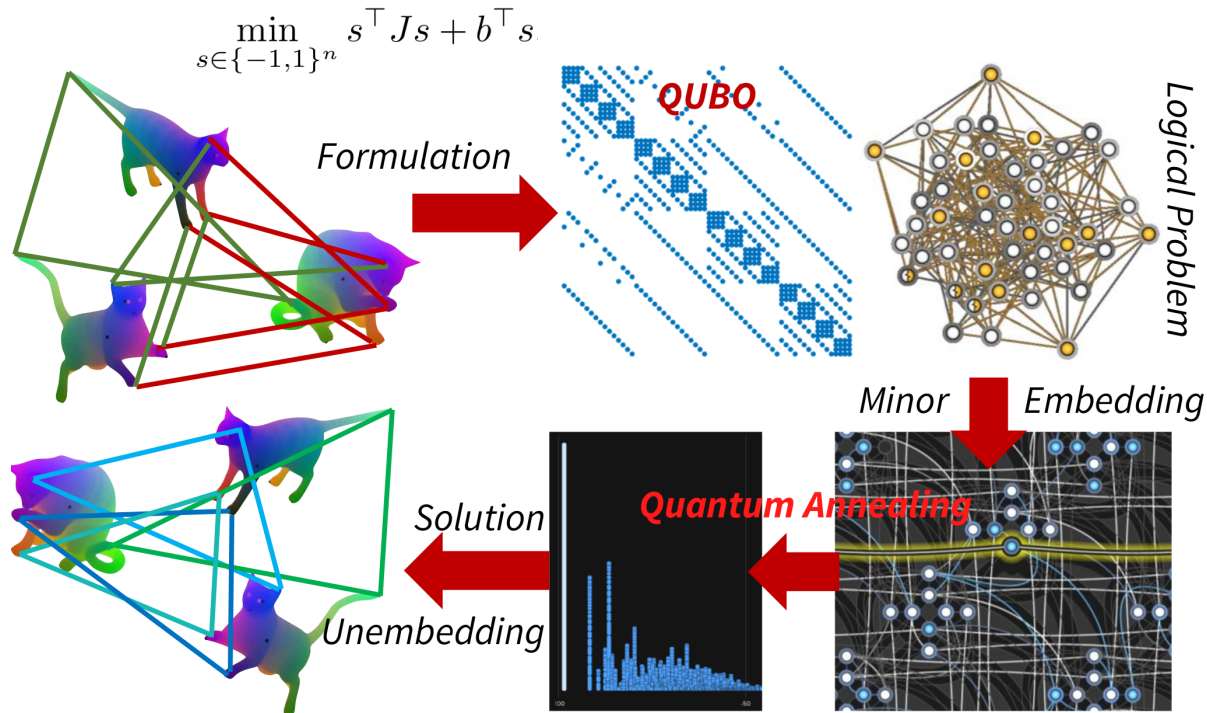
Adiabatic Quantum Algorithms



Every AQC algorithm includes six steps:

- 1) **QUBO preparation**
- 2) Minor embedding
- 3) **Quantum annealing (sampling)**
- 4) Unembedding
- 5) Bitstring selection
- 6) Solution interpretation

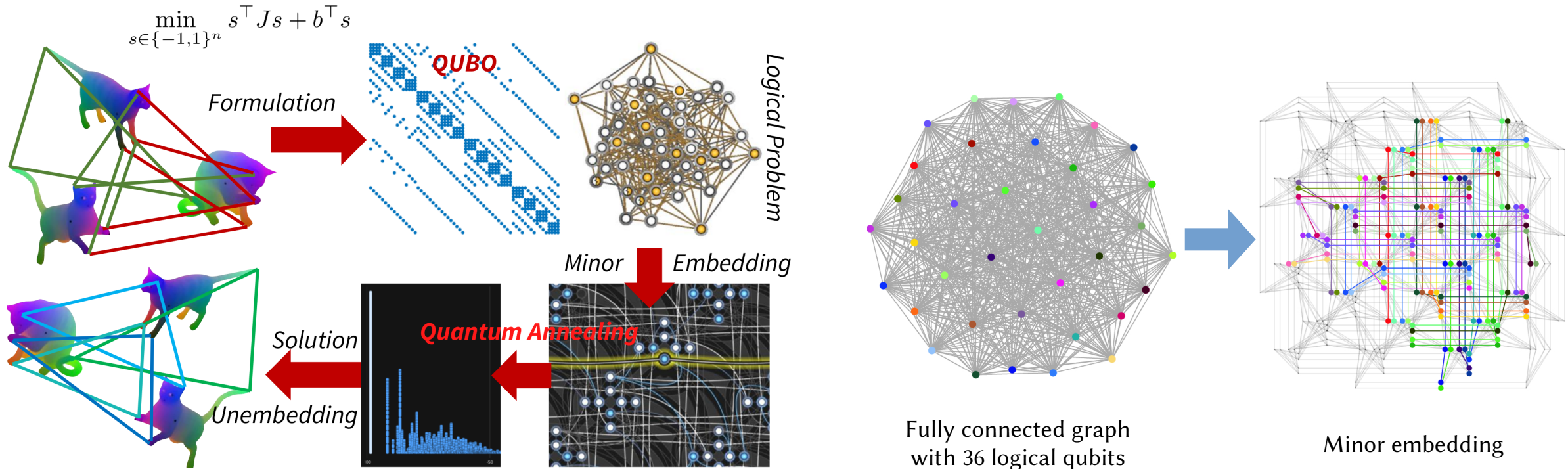
Adiabatic Quantum Algorithms



Every AQC algorithm includes six steps:

- 1) **QUBO preparation**
- 2) Minor embedding
- 3) **Quantum annealing (sampling)**
- 4) Unembedding
- 5) Bitstring selection
- 6) Solution interpretation

Adiabatic Quantum Algorithms



Every AQC algorithm includes six steps:

- 1) **QUBO preparation**
- 2) Minor embedding
- 3) **Quantum annealing (sampling)**
- 4) Unembedding
- 5) Bitstring selection
- 6) Solution interpretation

Quantum Computer Vision

3-Satisfiability	3D image tomography
Bayesian inference in imaging	Binary matrix factorization
Budget pacing in auctions	Calibrating transmissions
Capacitated vehicle routing	Chemical structure analysis
Designing metamaterials	Display advertisement optimization
Donor-patient matching	Election modeling
Factoring	Factory vehicle scheduling
Fault diagnosis	Fault tree analysis
Financial stress analysis	Flight gate assignment
IMRT beamlet optimization	Job-shop scheduling
Linear least squares	List order optimization
Detecting LHC particle collisions	MIMO processing in radio networks
Minimizing polynomials	Modeling molecular dynamics
Model predictive control	Modeling terrorist networks
Number partitioning	Peptide design
Phylogenetics	Portfolio optimization
Satellite scheduling	Simulating KT phase transitions
Simulating material structures	Simulating atomic magnetometers
Simulating quantum lattice transitions	Stock market forecasting
Telecommunications network design	Topological data analysis
Traffic flow optimization	Traffic signal optimization
Tsunami evacuation routing	Waste collection optimization
ML: accelerating deep learning	ML: classification in cancer research
ML: classification in DNA analysis	ML: quantum boosting
ML: training neural networks	ML: reinforcement learning
ML: unsupervised learning	

Quantum Computer Vision

3-Satisfiability	3D image tomography
Bayesian inference in imaging	Binary matrix factorization
Budget pacing in auctions	Calibrating transmissions
Capacitated vehicle routing	Chemical structure analysis
Designing metamaterials	Display advertisement optimization
Donor-patient matching	Election modeling
Factoring	Factory vehicle scheduling
Fault diagnosis	Fault tree analysis
Financial stress analysis	Flight gate assignment
IMRT beamlet optimization	Job-shop scheduling
Linear least squares	List order optimization
Detecting LHC particle collisions	MIMO processing in radio networks
Minimizing polynomials	Modeling molecular dynamics
Model predictive control	Modeling terrorist networks
Number partitioning	Peptide design
Phylogenetics	Portfolio optimization
Satellite scheduling	Simulating KT phase transitions
Simulating material structures	Simulating atomic magnetometers
Simulating quantum lattice transitions	Stock market forecasting
Telecommunications network design	Topological data analysis
Traffic flow optimization	Traffic signal optimization
Tsunami evacuation routing	Waste collection optimization
ML: accelerating deep learning	ML: classification in cancer research
ML: classification in DNA analysis	ML: quantum boosting
ML: training neural networks	ML: reinforcement learning
ML: unsupervised learning	

Computer Vision and Graphics

Transformation estimation (2D, 3D)

Point set alignment

Graph matching

Permutation synchronisation

Non-rigid shape alignment

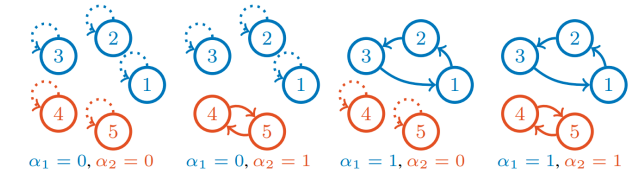
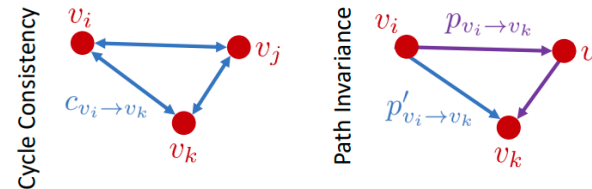
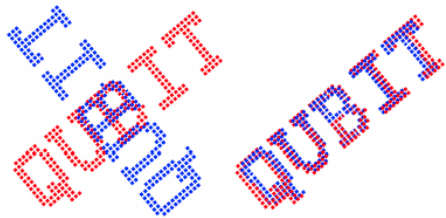
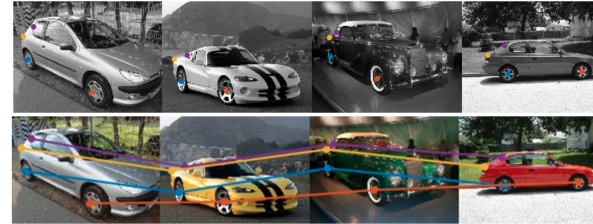
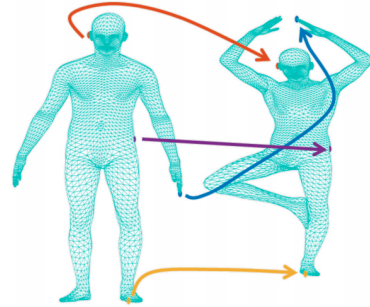
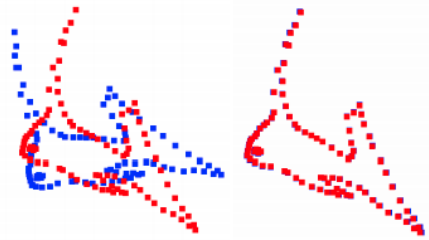
Motion segmentation

...

?

$$\min_{s \in \{-1, 1\}^n} s^\top J s + b^\top s$$

Quantum Computer Vision



Point set registration,
CVPR 2020

Graph matching,
3DV 2020

Permutation synchronisation,
CVPR 2021

Non-rigid shape alignment,
ICCV 2021

Golyanik and Theobalt. A Quantum Computational Approach to Correspondence Problems on Point Sets. *CVPR*, 2020.

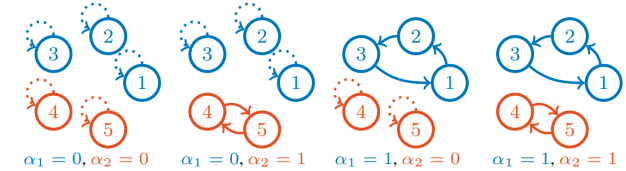
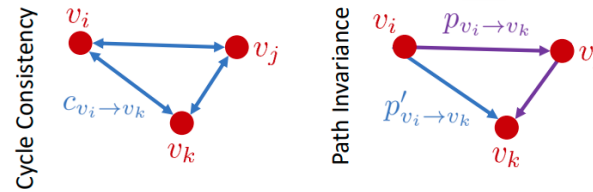
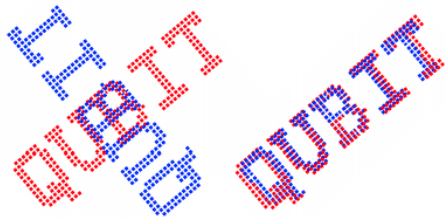
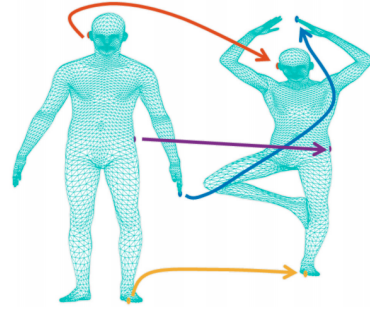
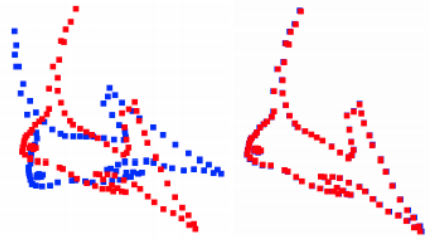
Seelbach Benkner, Golyanik, Theobalt, Moeller. Adiabatic Quantum Graph Matching with Permutation Matrix Constraints. *3DV*, 2020.

Birdal*, Golyanik*, Theobalt, Guibas. Quantum Permutation Synchronization. *CVPR*, 2021.

* equal contribution

Seelbach Benkner, Löhner, Golyanik, Wunderlich, Theobalt, Moeller. Q-Match: Iterative Shape Matching via Quantum Annealing. *ICCV*, 2021.

Quantum Computer Vision



Point set registration,
CVPR 2020

Graph matching,
3DV 2020

Permutation synchronisation,
CVPR 2021

Non-rigid shape alignment,
ICCV 2021

Golyanik and Theobalt. A Quantum Computational Approach to Correspondence Problems on Point Sets. *CVPR*, 2020.

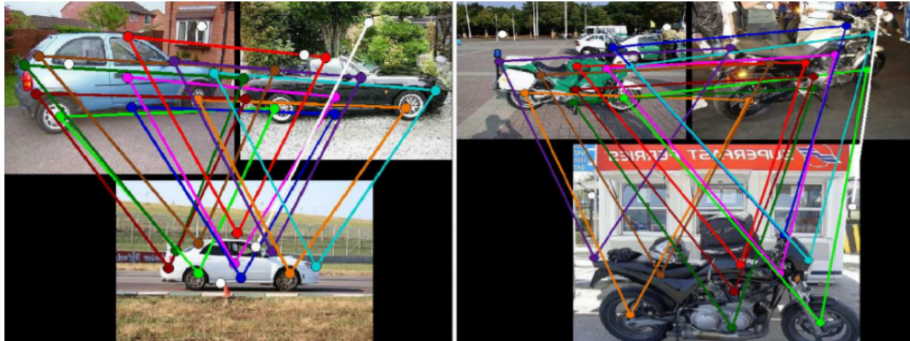
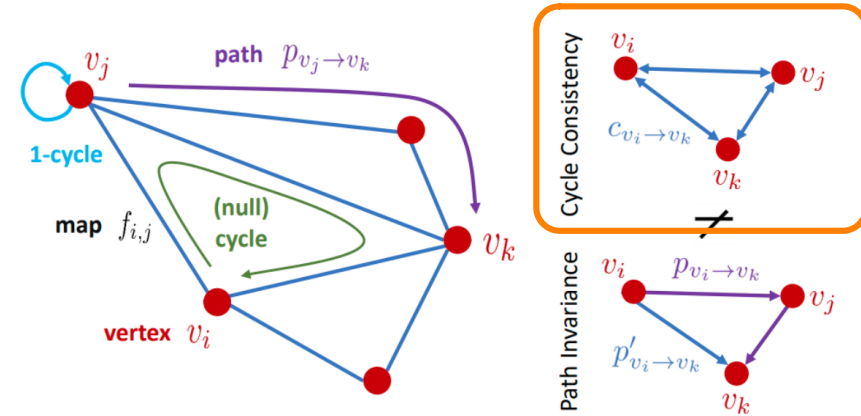
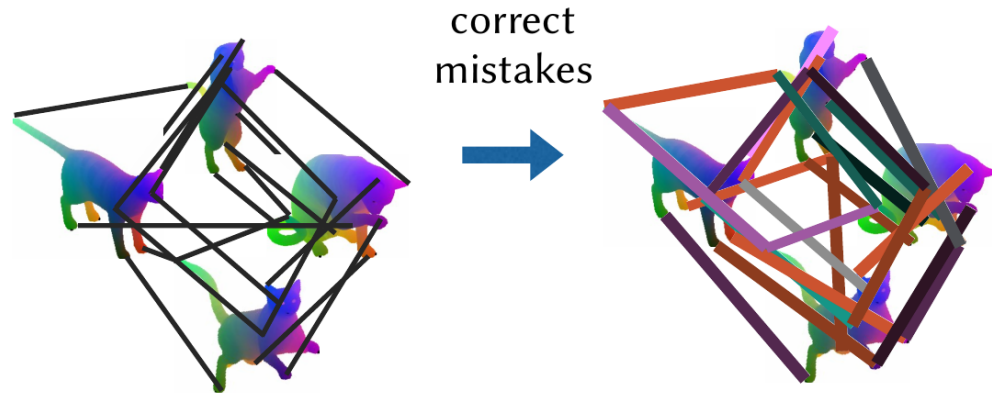
Seelbach Benkner, Golyanik, Theobalt, Moeller. Adiabatic Quantum Graph Matching with Permutation Matrix Constraints. *3DV*, 2020.

Birdal*, Golyanik*, Theobalt, Guibas. Quantum Permutation Synchronization. *CVPR*, 2021.

* equal contribution

Seelbach Benkner, Löhner, Golyanik, Wunderlich, Theobalt, Moeller. Q-Match: Iterative Shape Matching via Quantum Annealing. *ICCV*, 2021.

Quantum Permutation Synchronisation



2D or 3D inputs



$$\arg \min_{\mathbf{x} \in \mathcal{B}^n} \mathbf{x}^\top \mathbf{Q} \mathbf{x} + \mathbf{s}^\top \mathbf{x}$$

Binary Variables Quadratic Term Linear Term

Quantum Permutation Synchronisation

$$\arg \min_{\{\mathbf{X}_i \in \mathcal{P}_n\}} \sum_{(i,j) \in \mathcal{E}} \|\mathbf{P}_{ij} - \mathbf{X}_i \mathbf{X}_j^\top\|_{\mathbb{F}}^2 = \arg \min_{\{\mathbf{X}_i \in \mathcal{P}_n\}} \mathbf{x}^\top \mathbf{Q}' \mathbf{x},$$

$$\mathbf{Q}' = - \begin{bmatrix} \mathbf{I} \otimes \mathbf{P}_{11} & \mathbf{I} \otimes \mathbf{P}_{12} & \cdots & \mathbf{I} \otimes \mathbf{P}_{1m} \\ \mathbf{I} \otimes \mathbf{P}_{21} & \mathbf{I} \otimes \mathbf{P}_{22} & \cdots & \mathbf{I} \otimes \mathbf{P}_{2m} \\ \vdots & \vdots & \ddots & \vdots \\ \mathbf{I} \otimes \mathbf{P}_{m1} & \mathbf{I} \otimes \mathbf{P}_{m2} & \cdots & \mathbf{I} \otimes \mathbf{P}_{mm} \end{bmatrix}.$$

Quantum Permutation Synchronisation

$$\arg \min_{\{\mathbf{X}_i \in \mathcal{P}_n\}} \sum_{(i,j) \in \mathcal{E}} \|\mathbf{P}_{ij} - \mathbf{X}_i \mathbf{X}_j^\top\|_{\mathbb{F}}^2 = \arg \min_{\{\mathbf{X}_i \in \mathcal{P}_n\}} \mathbf{x}^\top \mathbf{Q}' \mathbf{x},$$

$$\arg \min_{\mathbf{x} \in \mathcal{B}} \mathbf{x}^\top \mathbf{Q}' \mathbf{x} \quad s.t. \quad \mathbf{A} \mathbf{x} = \mathbf{b}$$

$$\mathbf{Q}' = - \begin{bmatrix} \mathbf{I} \otimes \mathbf{P}_{11} & \mathbf{I} \otimes \mathbf{P}_{12} & \cdots & \mathbf{I} \otimes \mathbf{P}_{1m} \\ \mathbf{I} \otimes \mathbf{P}_{21} & \mathbf{I} \otimes \mathbf{P}_{22} & \cdots & \mathbf{I} \otimes \mathbf{P}_{2m} \\ \vdots & \vdots & \ddots & \vdots \\ \mathbf{I} \otimes \mathbf{P}_{m1} & \mathbf{I} \otimes \mathbf{P}_{m2} & \cdots & \mathbf{I} \otimes \mathbf{P}_{mm} \end{bmatrix}.$$

is turned into

$$\arg \min_{\mathbf{x} \in \mathcal{B}} \mathbf{x}^\top \mathbf{Q} \mathbf{x} + \mathbf{s}^\top \mathbf{x},$$

where $\mathbf{Q} = \mathbf{Q}' + \lambda \mathbf{A}^\top \mathbf{A}$ and $\mathbf{s} = -2\lambda \mathbf{A}^\top \mathbf{b}$.

Quantum Permutation Synchronisation

$$\arg \min_{\{\mathbf{X}_i \in \mathcal{P}_n\}} \sum_{(i,j) \in \mathcal{E}} \|\mathbf{P}_{ij} - \mathbf{X}_i \mathbf{X}_j^\top\|_F^2 = \arg \min_{\{\mathbf{X}_i \in \mathcal{P}_n\}} \mathbf{x}^\top \mathbf{Q}' \mathbf{x},$$

$$\arg \min_{\mathbf{x} \in \mathcal{B}} \mathbf{x}^\top \mathbf{Q}' \mathbf{x} \quad s.t. \quad \mathbf{A} \mathbf{x} = \mathbf{b}$$

$$\mathbf{Q}' = - \begin{bmatrix} \mathbf{I} \otimes \mathbf{P}_{11} & \mathbf{I} \otimes \mathbf{P}_{12} & \cdots & \mathbf{I} \otimes \mathbf{P}_{1m} \\ \mathbf{I} \otimes \mathbf{P}_{21} & \mathbf{I} \otimes \mathbf{P}_{22} & \cdots & \mathbf{I} \otimes \mathbf{P}_{2m} \\ \vdots & \vdots & \ddots & \vdots \\ \mathbf{I} \otimes \mathbf{P}_{m1} & \mathbf{I} \otimes \mathbf{P}_{m2} & \cdots & \mathbf{I} \otimes \mathbf{P}_{mm} \end{bmatrix}.$$

is turned into

$$\arg \min_{\mathbf{x} \in \mathcal{B}} \mathbf{x}^\top \mathbf{Q} \mathbf{x} + \mathbf{s}^\top \mathbf{x},$$

where $\mathbf{Q} = \mathbf{Q}' + \lambda \mathbf{A}^\top \mathbf{A}$ and $\mathbf{s} = -2\lambda \mathbf{A}^\top \mathbf{b}$.

$$\mathcal{P}_n := \{ \mathbf{P} \in \underbrace{\{0, 1\}^{n \times n}}_{\text{Binary}} : \underbrace{\mathbf{P} \mathbf{1}_n = \mathbf{1}_n}_{\text{Rows sum to 1}}, \underbrace{\mathbf{1}_n^\top \mathbf{P} = \mathbf{1}_n^\top}_{\text{Cols sum to 1}} \}$$

$$\mathbf{A}_i = \begin{bmatrix} \mathbf{I} \otimes \mathbf{1}^\top \\ \mathbf{1}^\top \otimes \mathbf{I} \end{bmatrix} \quad \longrightarrow \quad \mathbf{A} = \begin{bmatrix} \mathbf{A}_1 & & & \\ & \mathbf{A}_2 & & \\ & & \ddots & \\ & & & \mathbf{A}_n \end{bmatrix}$$

$$\mathbf{b}_i = \mathbf{1} \quad \mathbf{b} = \mathbf{1}$$

Quantum Permutation Synchronisation

$$\arg \min_{\{\mathbf{X}_i \in \mathcal{P}_n\}} \sum_{(i,j) \in \mathcal{E}} \|\mathbf{P}_{ij} - \mathbf{X}_i \mathbf{X}_j^\top\|_F^2 = \arg \min_{\{\mathbf{X}_i \in \mathcal{P}_n\}} \mathbf{x}^\top \mathbf{Q}' \mathbf{x},$$

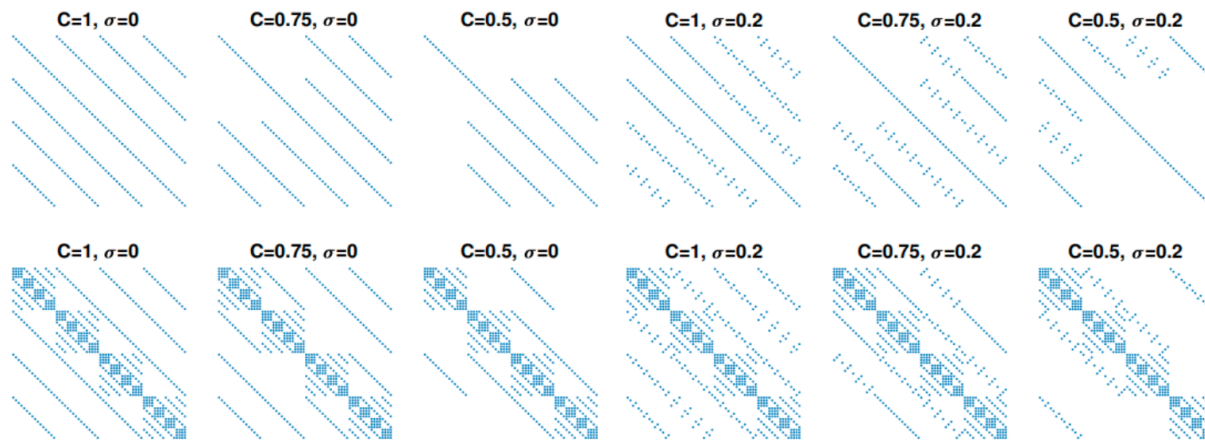
$$\arg \min_{\mathbf{x} \in \mathcal{B}} \mathbf{x}^\top \mathbf{Q}' \mathbf{x} \quad s.t. \quad \mathbf{A} \mathbf{x} = \mathbf{b}$$

$$\mathbf{Q}' = - \begin{bmatrix} \mathbf{I} \otimes \mathbf{P}_{11} & \mathbf{I} \otimes \mathbf{P}_{12} & \cdots & \mathbf{I} \otimes \mathbf{P}_{1m} \\ \mathbf{I} \otimes \mathbf{P}_{21} & \mathbf{I} \otimes \mathbf{P}_{22} & \cdots & \mathbf{I} \otimes \mathbf{P}_{2m} \\ \vdots & \vdots & \ddots & \vdots \\ \mathbf{I} \otimes \mathbf{P}_{m1} & \mathbf{I} \otimes \mathbf{P}_{m2} & \cdots & \mathbf{I} \otimes \mathbf{P}_{mm} \end{bmatrix}.$$

is turned into

$$\arg \min_{\mathbf{x} \in \mathcal{B}} \mathbf{x}^\top \mathbf{Q} \mathbf{x} + \mathbf{s}^\top \mathbf{x},$$

where $\mathbf{Q} = \mathbf{Q}' + \lambda \mathbf{A}^\top \mathbf{A}$ and $\mathbf{s} = -2\lambda \mathbf{A}^\top \mathbf{b}$.



Exemplary \mathbf{Q}

$$\mathcal{P}_n := \{ \mathbf{P} \in \{0, 1\}^{n \times n} : \underbrace{\mathbf{P} \mathbf{1}_n = \mathbf{1}_n}_{\text{Binary}}, \underbrace{\mathbf{1}_n^\top \mathbf{P} = \mathbf{1}_n^\top}_{\text{Rows sum to 1}}, \underbrace{\mathbf{1}_n^\top \mathbf{P} = \mathbf{1}_n^\top}_{\text{Cols sum to 1}} \}$$

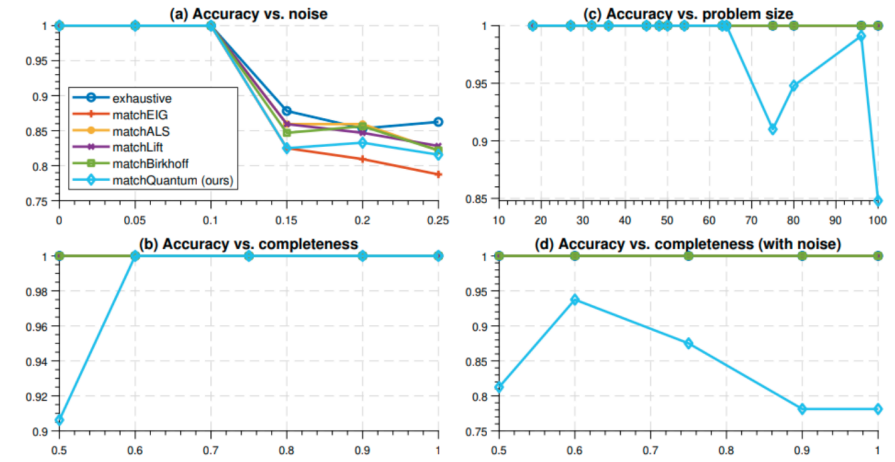
$$\mathbf{A}_i = \begin{bmatrix} \mathbf{I} \otimes \mathbf{1}^\top \\ \mathbf{1}^\top \otimes \mathbf{I} \end{bmatrix} \quad \Rightarrow \quad \mathbf{A} = \begin{bmatrix} \mathbf{A}_1 & & & \\ & \mathbf{A}_2 & & \\ & & \ddots & \\ & & & \mathbf{A}_n \end{bmatrix}$$

$\mathbf{b}_i = \mathbf{1} \quad \Rightarrow \quad \mathbf{b} = \mathbf{1}$

Quantum Permutation Synchronisation

	Car	Duck	Motorbike	Winebottle	Average
Exhaustive	0.84 ± 0.104	0.91 ± 0.115	0.82 ± 0.10	0.95 ± 0.096	0.88 ± 0.104
EIG	0.81 ± 0.083	0.86 ± 0.102	0.77 ± 0.059	0.87 ± 0.107	0.83 ± 0.088
ALS	0.84 ± 0.095	0.90 ± 0.102	0.81 ± 0.078	0.94 ± 0.092	0.87 ± 0.092
LIFT	0.84 ± 0.102	0.90 ± 0.103	0.81 ± 0.078	0.94 ± 0.092	0.87 ± 0.094
Birkhoff	0.84 ± 0.094	0.90 ± 0.107	0.81 ± 0.079	0.94 ± 0.093	0.87 ± 0.093
D-Wave(Ours)	0.84 ± 0.104	0.90 ± 0.104	0.81 ± 0.080	0.93 ± 0.095	0.87 ± 0.096

Average Errors

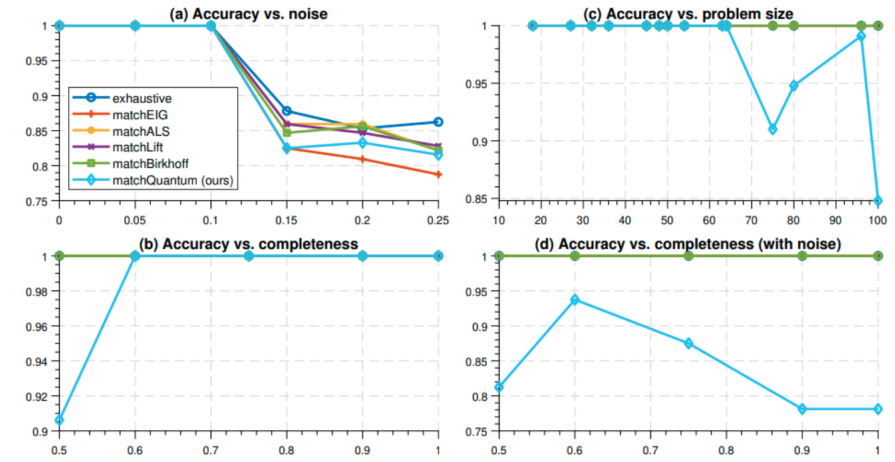
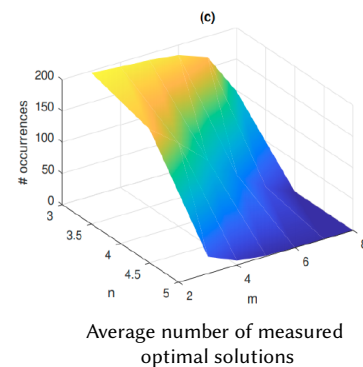
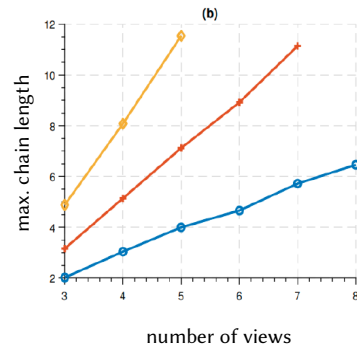
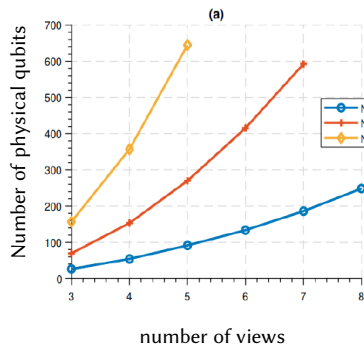


Evaluations on the synthetic dataset (4 views and 4 points)

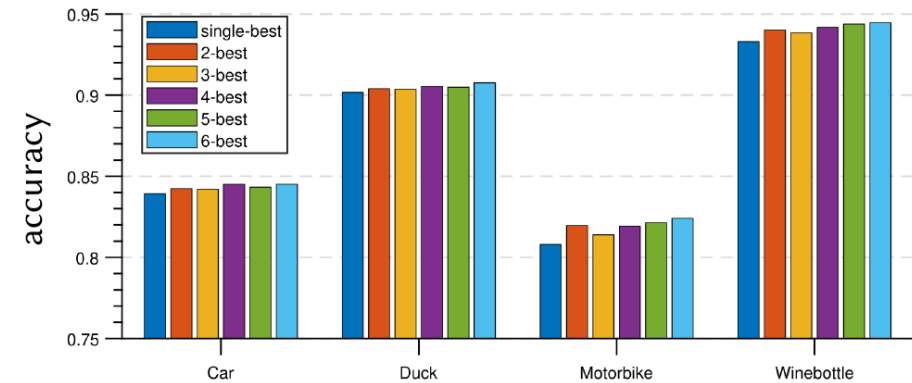
Quantum Permutation Synchronisation

	Car	Duck	Motorbike	Winebottle	Average
Exhaustive	0.84 ± 0.104	0.91 ± 0.115	0.82 ± 0.10	0.95 ± 0.096	0.88 ± 0.104
EIG	0.81 ± 0.083	0.86 ± 0.102	0.77 ± 0.059	0.87 ± 0.107	0.83 ± 0.088
ALS	0.84 ± 0.095	0.90 ± 0.102	0.81 ± 0.078	0.94 ± 0.092	0.87 ± 0.092
LIFT	0.84 ± 0.102	0.90 ± 0.103	0.81 ± 0.078	0.94 ± 0.092	0.87 ± 0.094
Birkhoff	0.84 ± 0.094	0.90 ± 0.107	0.81 ± 0.079	0.94 ± 0.093	0.87 ± 0.093
D-Wave(Ours)	0.84 ± 0.104	0.90 ± 0.104	0.81 ± 0.080	0.93 ± 0.095	0.87 ± 0.096

Average Errors

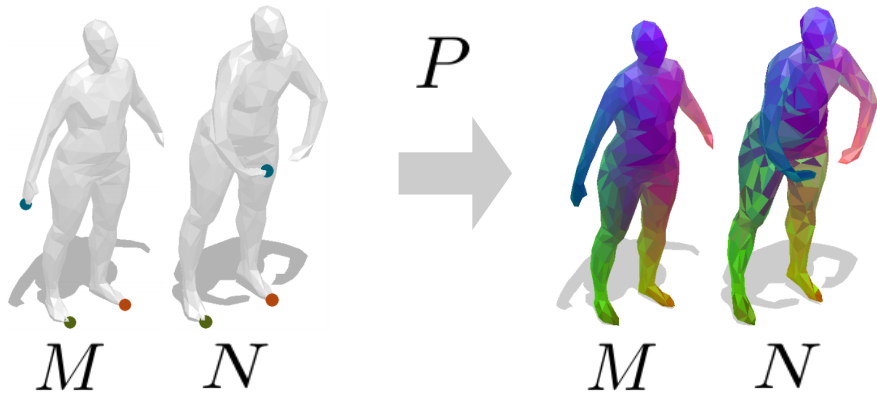


Evaluations on the synthetic dataset (4 views and 4 points)

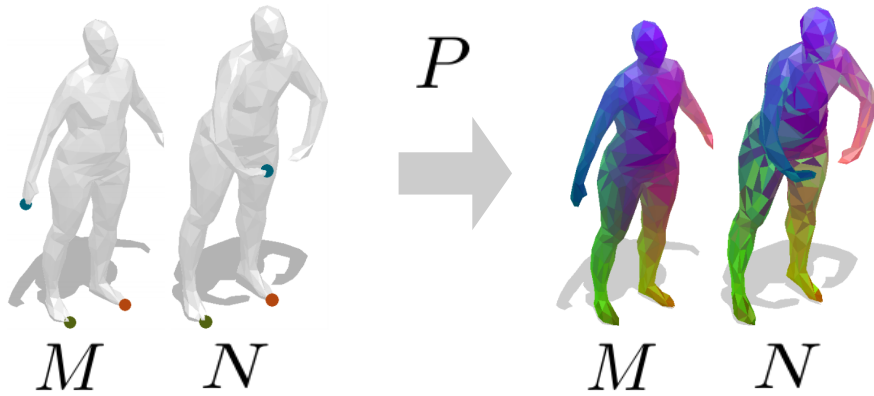


Bit corrections using multiple measurements of different energies

Q-Match: Iterative Shape Alignment



Q-Match: Iterative Shape Alignment



$$\min_{X \in \mathbb{P}_n} E(X) := \mathbf{x}^T W \mathbf{x}$$

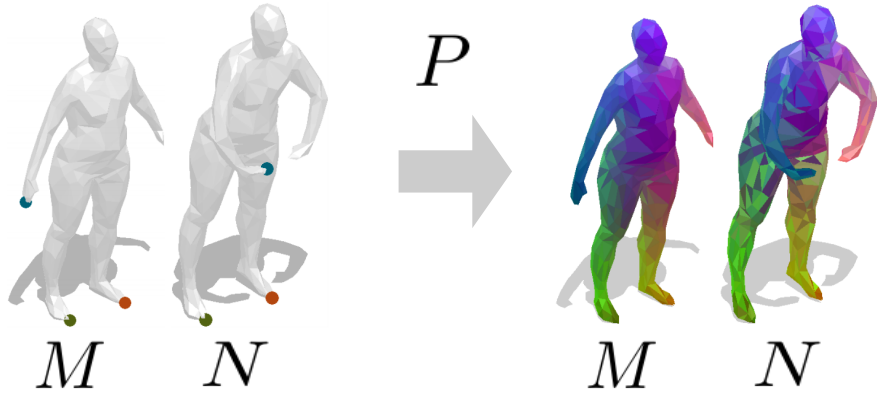
$$\mathbf{x} = \text{vec}(X) \quad W \in \mathbb{R}^{n^2 \times n^2}$$

$$\mathbb{P} \subset \{0, 1\}^{n \times n} \quad (\text{permutation matrix})$$

$$\mathbb{P}_n = \{X \in \{0, 1\}^{n \times n} \mid \sum_i X_{ij} = 1, \sum_j X_{ij} = 1 \forall i, j\}.$$



Q-Match: Iterative Shape Alignment



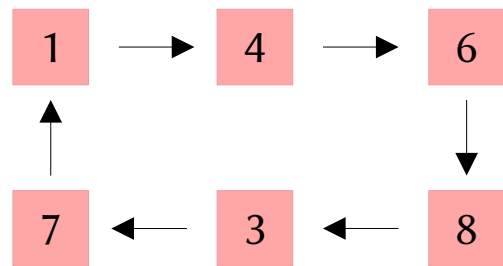
$$\min_{X \in \mathbb{P}_n} E(X) := \mathbf{x}^T W \mathbf{x}$$

$$\mathbf{x} = \text{vec}(X) \quad W \in \mathbb{R}^{n^2 \times n^2}$$

$$\mathbb{P} \subset \{0, 1\}^{n \times n} \quad (\text{permutation matrix})$$

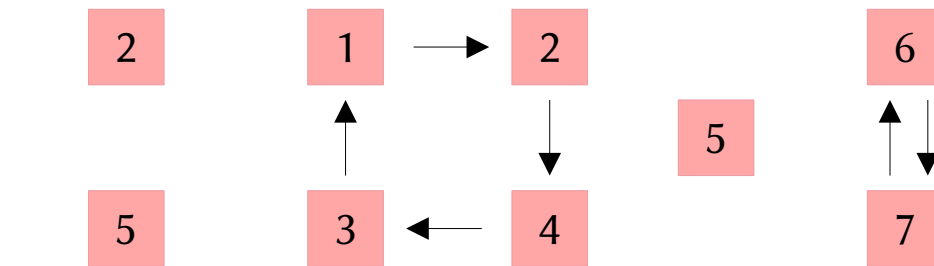
$$\mathbb{P}_n = \{X \in \{0, 1\}^{n \times n} \mid \sum_i X_{ij} = 1, \sum_j X_{ij} = 1 \forall i, j\}.$$

k-cycles:



six-cycle

Disjoint permutations commute:



fixed points

four-cycle

fixed point

two-cycle

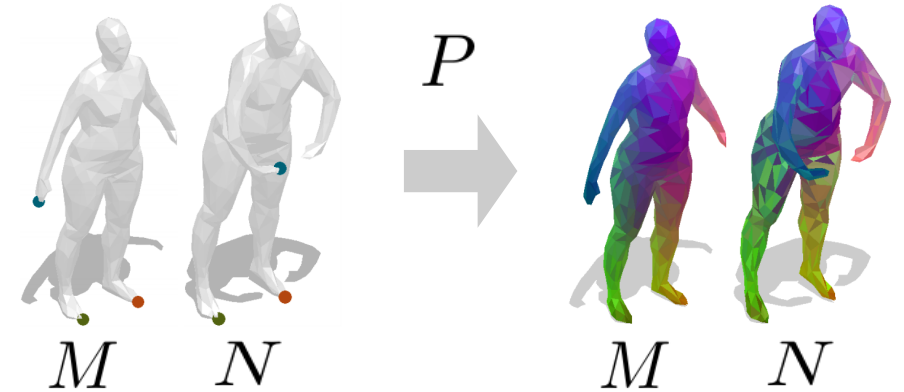
Any X can be written as $X = \prod_{i=0}^N C_i$,
i.e., a product of 2-cycles
(or, generally, disjoint k -cycles).

Q-Match: Iterative Shape Alignment

Given: 3D shapes M and N , both discretised with n vertices.

$$W_{i \cdot n + k, j \cdot n + l} = |d_M^g(i, j) - d_N^g(k, l)|$$

Find: optimal P

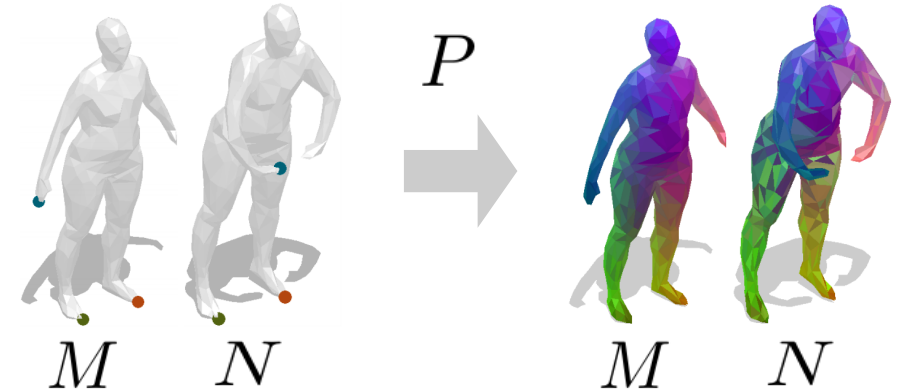


Q-Match: Iterative Shape Alignment

Given: 3D shapes M and N , both discretised with n vertices.

$$W_{i \cdot n + k, j \cdot n + l} = |d_M^g(i, j) - d_N^g(k, l)|$$

Find: optimal P



Want to solve but cannot:

$$\min_{X \in \mathbb{P}_n} E(X) := \mathbf{x}^T W \mathbf{x}$$

$$W_{i \cdot n + k, j \cdot n + l} = |d_M^g(i, j) - d_N^g(k, l)|$$

Instead solve

$$\arg \min_{\{P \in \mathbb{P}_n \mid \exists \alpha \in \{0, 1\}^m : P = (\prod_i c_i^{\alpha_i}) P_0\}} E(P)$$

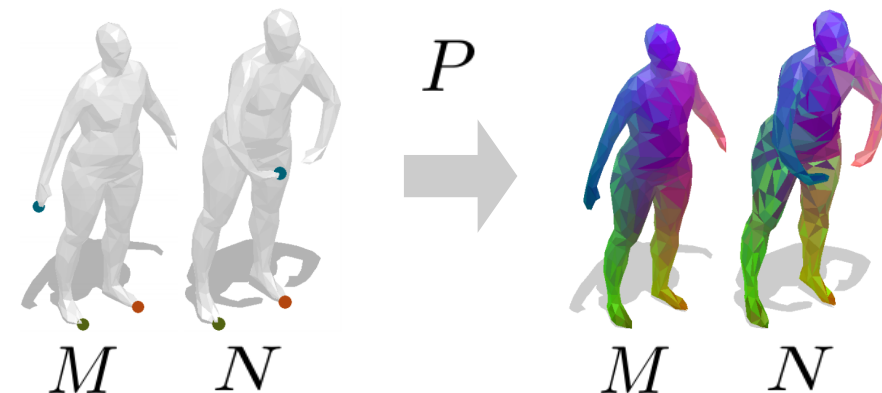
$$C = \{c_1, \dots, c_m\}$$

Q-Match: Iterative Shape Alignment

Given: 3D shapes M and N , both discretised with n vertices.

$$W_{i \cdot n + k, j \cdot n + l} = |d_M^g(i, j) - d_N^g(k, l)|$$

Find: optimal P



Want to solve but cannot:

$$\min_{X \in \mathbb{P}_n} E(X) := \mathbf{x}^T W \mathbf{x}$$

$$W_{i \cdot n + k, j \cdot n + l} = |d_M^g(i, j) - d_N^g(k, l)|$$

... leading to

$$\min_{\alpha \in \{0,1\}^m} \alpha^T \tilde{W} \alpha$$

$$\tilde{W}_{ij} = \begin{cases} E(C_i, C_j) & \text{if } i \neq j, \\ E(C_i, C_i) + E(C_i, P_0) + E(P_0, C_j) & \text{otherwise.} \end{cases}$$

not submodular

Instead solve

$$\arg \min_{\{P \in \mathbb{P}_n \mid \exists \alpha \in \{0,1\}^m: P = (\prod_i c_i^{\alpha_i}) P_0\}} E(P)$$

$$C = \{c_1, \dots, c_m\}$$

$$E(Q, R) = \text{vec}(Q)^T W \text{vec}(R)$$

$$P(\alpha) = P_0 + \sum_{i=1}^m \frac{\alpha_i (c_i - I) P_0}{C_i}$$

Q-Match: Iterative Shape Alignment

Assume $C = \{c_1, \dots, c_m\}$ is a set of disjoint cycles.

Consider

$$\begin{array}{c}
 \arg \min \\
 \{P \in \mathbb{P}_n \mid \exists \alpha \in \{0,1\}^m : P = (\prod_i c_i^{\alpha_i}) P_0\} \\
 \downarrow \qquad \qquad \qquad \searrow \\
 \text{binary vector parametrising } P \qquad \text{initial permutation } E(P)
 \end{array}$$

$$\begin{pmatrix}
 1-\alpha_1 & 0 & \alpha_1 & 0 & 0 \\
 \alpha_1 & 1-\alpha_1 & 0 & 0 & 0 \\
 0 & \alpha_1 & 1-\alpha_1 & 0 & 0 \\
 0 & 0 & 0 & 1-\alpha_2 & \alpha_2 \\
 0 & 0 & 0 & \alpha_2 & 1-\alpha_2
 \end{pmatrix}$$

Parametrisation of all combinations with two binary variables

Q-Match: Iterative Shape Alignment

Assume $C = \{c_1, \dots, c_m\}$ is a set of disjoint cycles.

Consider

$$\arg \min_{\{P \in \mathbb{P}_n \mid \exists \alpha \in \{0,1\}^m : P = (\prod_i c_i^{\alpha_i}) P_0\}} E(P)$$

binary vector parametrising P
initial permutation

$$\begin{pmatrix} 1-\alpha_1 & 0 & \alpha_1 & 0 & 0 \\ \alpha_1 & 1-\alpha_1 & 0 & 0 & 0 \\ 0 & \alpha_1 & 1-\alpha_1 & 0 & 0 \\ 0 & 0 & 0 & 1-\alpha_2 & \alpha_2 \\ 0 & 0 & 0 & \alpha_2 & 1-\alpha_2 \end{pmatrix}$$

Parametrisation of all combinations with two binary variables

$$\min_{X \in \mathbb{P}_n} E(X) := \mathbf{x}^T W \mathbf{x}$$

Initial QAP formulation;
cannot be solved on QPU

W initial matrix of costs; large; cannot be precomputed and stored; its entries are computed on demand in each iteration

$$\min_{\alpha \in \{0,1\}^m} \alpha^T \tilde{W} \alpha$$

QUBO formulation based on cyclic alpha-expansion; can be solved on QPU

\tilde{W} matrix of QUBO costs; requires known W

W_s a $k^2 \times k^2$ reduction of W based on k worst matches

Q-Match: Iterative Shape Alignment

Initialise P_0 via descriptor-based similarity

repeat until converged

obtain I_M and I_N and choose from them a set of k random and disjoint 2-cycles

construct a submatrix of worst matches W_s

repeat until every 2-cycle occurred

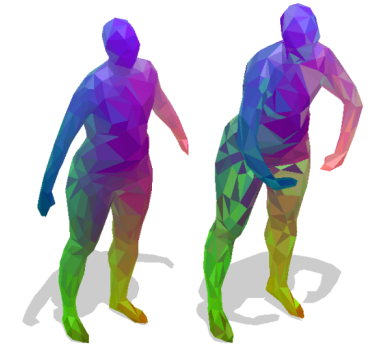
choose a random set of 2-cycles

calculate \tilde{W} and solve $\min_{\alpha \in \{0,1\}^m} \alpha^\top \tilde{W} \alpha$ on QPU

$$P_i = \left(\prod_j c_j^{\alpha_j} \right) P_{i-1}$$

apply the obtained permutation to worst matches

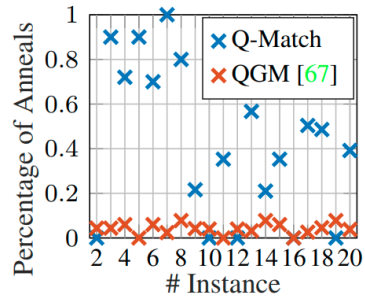
NP-hard; decides
to apply C_i or not



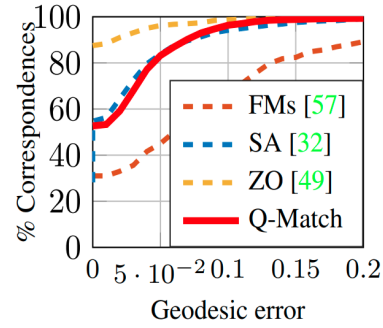
M N



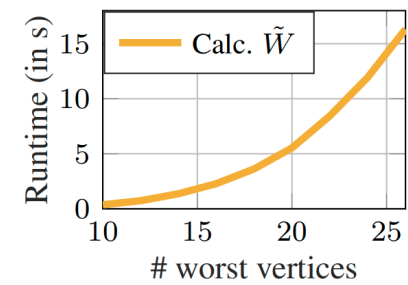
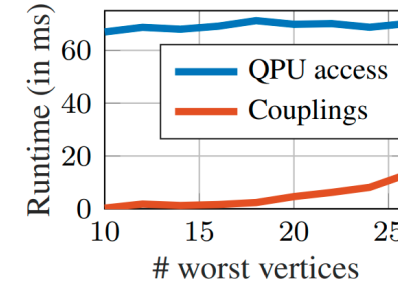
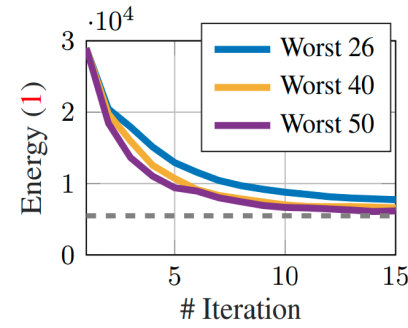
Q-Match: Iterative Shape Alignment



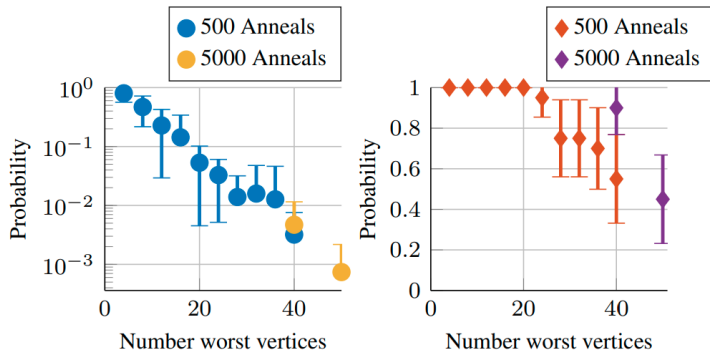
Retrieving the optimum



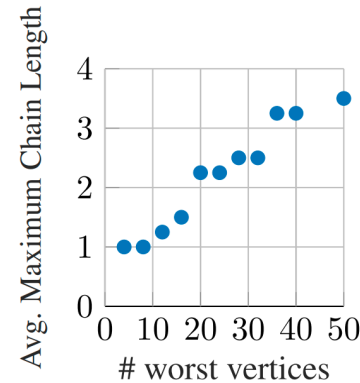
Cumulative error and convergence (FAUST)



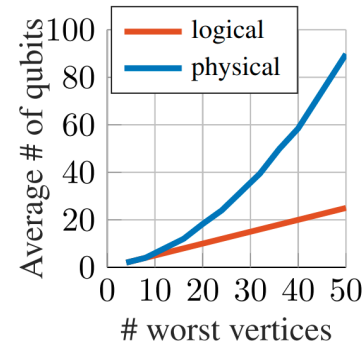
Runtime analysis



Success probabilities



Minor embedding functions



Exemplary minor embeddings
(using 40 and 50 worst vertices)

- [32] Holzschuh *et al.* Simulated annealing for 3d shape correspondence. *3DV*, 2020.
- [49] Melzi *et al.* Zoomout: Spectral upsampling for efficient shape correspondence. *ACM ToG*, 2019.
- [57] Ovsjanikov *et al.* Functional maps: a flexible representation of maps between shapes. *ACM ToG*, 2012.
- [67] Seelbach Benkner *et al.* Adiabatic Quantum Graph Matching with Permutation Matrix Constraints. *3DV*, 2020.

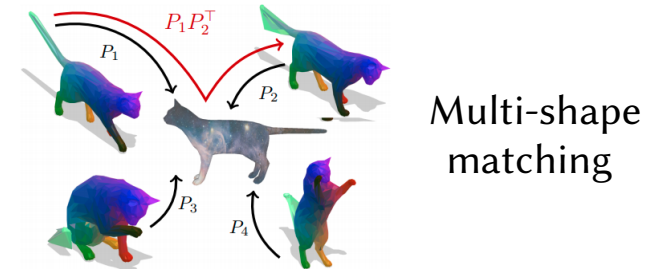
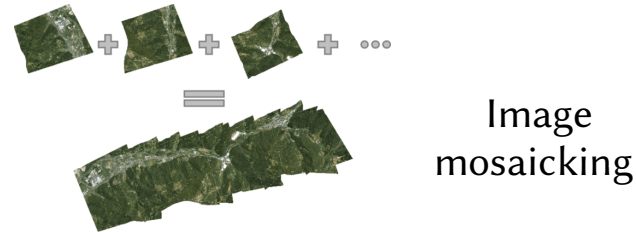
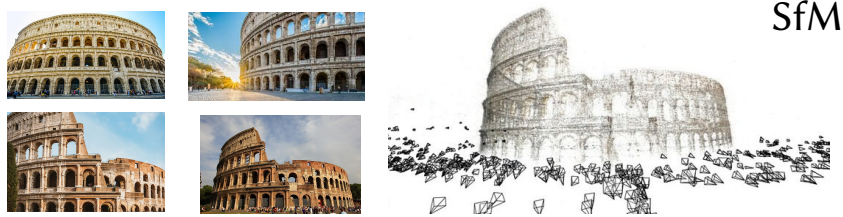
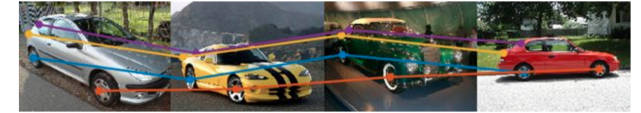
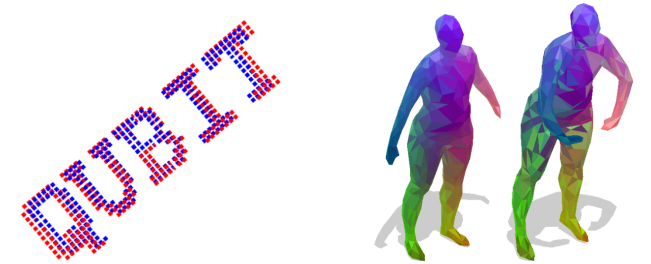
Conclusions and Open Challenges

- Problem types: matching and synchronisation
- Input data: pairwise permutations, point sets, graphs, meshes
- Competitive results for small problems (if solved as a single QUBO sampling) and real-world problems (an iterative CPU-QPU policy)
- Iterative policies with CPU-QPU tasks are promising
- Runtime of the state preparation (QUBO) is not negligible
- The proposed algorithms will improve with hardware improvements (2000Q vs Advantage system1.1)



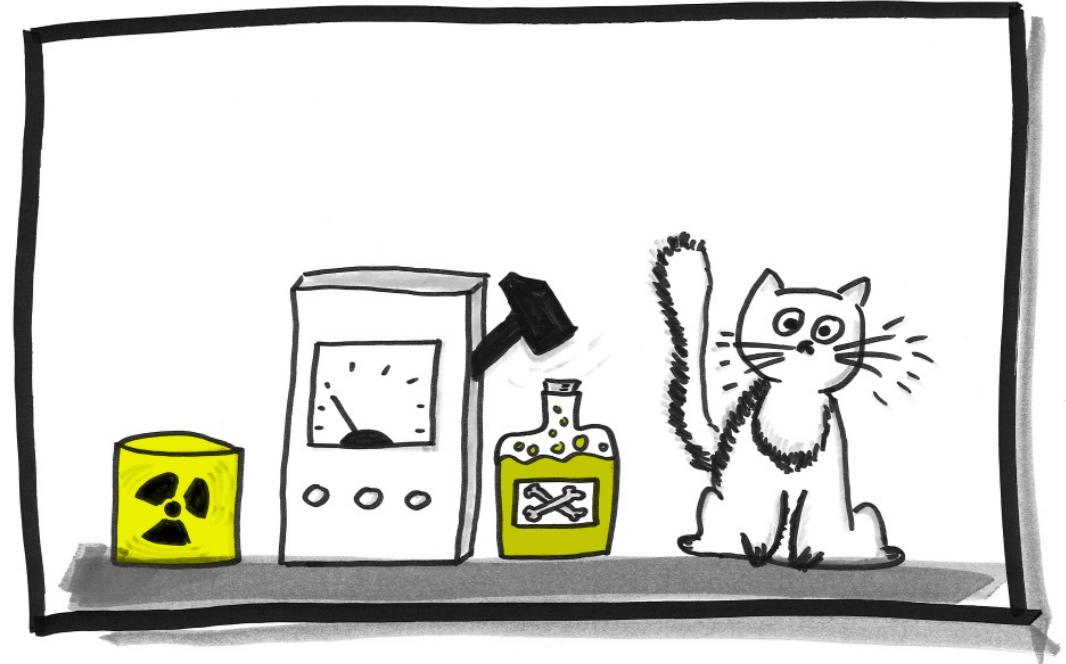
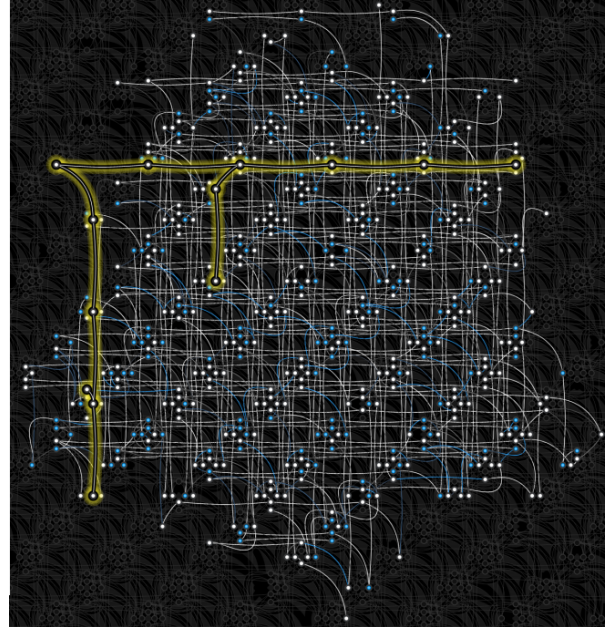
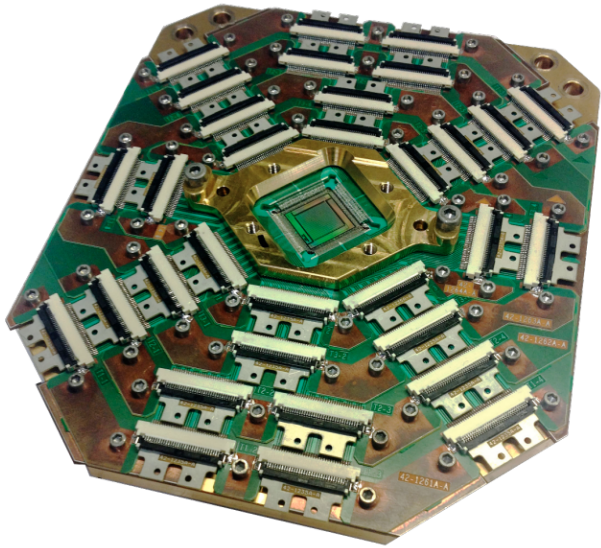
Conclusions and Open Challenges

- Problem types: matching and synchronisation
- Input data: pairwise permutations, point sets, graphs, meshes
- Competitive results for small problems (if solved as a single QUBO sampling) and real-world problems (an iterative CPU-QPU policy)
- Iterative policies with CPU-QPU tasks are promising
- Runtime of the state preparation (QUBO) is not negligible
- The proposed algorithms will improve with hardware improvements (2000Q vs Advantage system1.1)



- Many signs that quantum computing technology will continue developing next decades
- We are expecting to see works on quantum computer vision from more and more research groups
- Related research fields: quantum machine learning, circuit-based QC algorithms

Questions?



Thank You!